

Characteristics and Trends of River Discharge into Hudson, James, and Ungava Bays, 1964-2000

Stephen J. Déry^{1,2}, Marc Stieglitz³, Edward C. McKenna⁴, and Eric F. Wood⁵

¹Lamont-Doherty Earth Observatory, Columbia University, Palisades, New York

²Program in Atmospheric and Oceanic Sciences, Princeton University
Princeton, New Jersey

³School of Civil and Environmental Engineering and School of Earth and
Atmospheric Sciences, Georgia Institute of Technology, Atlanta, Georgia

⁴Albertus Magnus High School, Bardonia, New York

⁵Department of Civil and Environmental Engineering, Princeton University
Princeton, New Jersey

Submitted in revised form to *Journal of Climate*

Reference # JCL-5103

December 6, 2004

Corresponding Author and Current Address:

Stephen J. Déry

Program in Atmospheric and Oceanic Sciences

Princeton University

307 GFDL

Princeton, NJ

08542

E-mail: sdery@princeton.edu

Abstract

The characteristics and trends of observed river discharge into Hudson, James, and Ungava Bays (HJUBs) for the period 1964-2000 are investigated. Forty-two rivers with outlets into these bays contribute on average $714 \text{ km}^3 \text{ yr}^{-1}$ ($=0.023 \text{ Sv}$) of freshwater to high-latitude oceans. For the system as a whole, discharge attains an annual peak of $4.2 \text{ km}^3 \text{ day}^{-1}$ on average in mid-June, whereas the minimum of $0.68 \text{ km}^3 \text{ day}^{-1}$ occurs on average during the last week of March. The Nelson River contributes as much as 34% of the daily discharge for the entire system during winter, but diminishes in relative importance during spring and summer. Runoff rates per contributing area are highest (lowest) on the eastern (western) shores of Hudson and James Bays. Linear trend analyses reveal decreasing discharge over the 37-year period in 36 out of the 42 rivers. By 2000, the total annual freshwater discharge into HJUBs diminished by 96 km^3 (-13%) from its value in 1964, equivalent to a reduction of 0.003 Sv . The annual peak discharge rates associated with snowmelt has advanced by nine days between 1964 and 2000 and has diminished by $0.036 \text{ km}^3 \text{ day}^{-1}$ in intensity. There is a direct correlation between the timing of peak spring discharge rates and the latitude of a river's mouth; the spring freshet varies by five days for each degree of latitude. Continental snowmelt induces a seasonal pulse of freshwater from HJUBs that is tracked along its path into the Labrador Current. It is suggested that the annual upper ocean salinity minimum observed on the inner Newfoundland Shelf can be explained by freshwater pulses composed of meltwater from three successive winter seasons in the river basins draining into HJUBs. A gradual salinization of the upper ocean during summer over the period 1966-94 on the inner Newfoundland Shelf is in accord with a decadal trend of a diminishing intensity in the continental meltwater pulses.

1. Introduction

Rivers provide a natural pathway for freshwater on the land surface and constitute a vital link between the atmosphere, the land surface, and the oceans. Streams and rivers integrate spatially and temporally atmospheric and land surface processes at the catchment-scale, providing a mechanism by which climate change may be detected. One area where significant climate change is ongoing is the Arctic (Serreze et al. 2000). Modifications to the high-latitude environment, driven by rising surface air temperatures (Chapman and Walsh 1993), include a decreasing depth and duration of the snowcover (Brown and Braaten 1998; Curtis et al. 1998), a warming and thawing of the permafrost (Osterkamp and Romanovsky 1996; Stieglitz et al. 2003), and increasing storminess and precipitation (McCabe et al. 2001; Walsh 2000). Such changes in the high-latitude environment all affect freshwater discharge in complex ways; however, given that river runoff is driven mainly by precipitation and surface air temperature, recent observations suggest an acceleration of the hydrological cycle in many northern regions, including increasing freshwater discharge (Peterson et al. 2002; Ziegler et al. 2003).

Historical discharge from the Canadian Mackenzie River Basin and from the three largest Siberian drainage basins (Yenisey, Lena, and Ob River Basins) are well sampled and documented (e.g., Stewart et al. 1998; Lammers et al. 2001; Peterson et al. 2002; Yang et al. 2002). By comparison, the Hudson, James, and Ungava Bays (HJUBs) drainage basin has received little attention. Unlike its major Russian and Canadian counterparts, the HJUBs basin consist of a large number of rivers with relatively lower runoff rates. For instance, the Yenisey, Lena, Ob, and Mackenzie Rivers supply no less than 50% of the annual freshwater discharge to the Arctic Ocean. The average annual runoff rates for these four large rivers attains \sim

500 km³ yr⁻¹, whereas the greatest annual discharge rate recorded for a single river flowing into HJUBs reaches only 70 km³ yr⁻¹ for the Nelson River (Carmack 2000). Yet the HJUBs drainage system alone equates 18% of the total discharge to the Arctic Ocean, more so than any other large river basin in Eurasia and North America (Shiklomanov et al. 2000). Variability and change in the discharge of freshwater into HJUBs has implications for the transport of nutrients, sediments, and other trace species to high-latitude oceans (Anderson et al. 2004), sea ice formation (Manak and Mysak 1989; Weatherly and Walsh 1996; Saucier and Dionne 1998; Saucier et al. 2004), and the thermohaline circulation (Aagaard and Carmack 1989).

Given the importance of the HJUBs drainage network in the global freshwater budget and the recent decline in the number of monitoring flow gauges in Canada (Shiklomanov et al. 2002), there is a critical need to report historical discharge rates of Canadian rivers with outlets into HJUBs. Furthermore, general circulation models forecast that the Hudson Bay region will experience some of the more dramatic environmental changes in the coming century (Gough and Wolfe 2001; Gagnon and Gough 2004). The main objective of this paper is to document the characteristics of freshwater discharge rates of 42 rivers that flow into HJUBs and to analyze the data for interannual variability and trends. The study period covers 37 years (1964-2000) when relatively good spatial and temporal coverage of river discharge data exists.

The paper is organized as follows: Section 2 provides background information on the HJUBs drainage basin and section 3 introduces the dataset and methods used in this study. Section 4 provides the analysis of our results that are compared in section 5 to other studies found in the literature. Section 6 discusses the implications of freshwater discharge into HJUBs on upper ocean salinity values in the Labrador Current. The paper closes in section 7 with a summary of our major findings and

plans for future work.

2. Study Area

The HJUBs covers an area of approximately 3.7×10^6 km², or more than one third of Canada (Fig. 1). The basin collects freshwater over 20° of latitude and over 50° of longitude. The provinces of Alberta, Saskatchewan, Manitoba, Ontario, and Québec, as well as Nunavut Territory, all contribute substantial freshwater to the HJUBs watershed. The American states of Montana, North Dakota, South Dakota, and Minnesota are also a source of freshwater for the HJUBs. Forty-two of the most important rivers that drain into HJUBs are listed in Table 1. These rivers are identified by one of the three bays into which they discharge, as well as the province or territory where their outlet in HJUBs is situated.

The mean annual air temperature of the HJUBs varies considerably from north to south, ranging from 4°C in the Canadian Prairies to -12°C in Nunavut (Table 2). The total mean annual precipitation exhibits latitudinal and longitudinal gradients. Average minima of ~ 300 mm are found in both extreme northern and southern sections of the drainage basin, whereas average maxima of ~ 800 mm are found at intermediate locations in the boreal forest. Annual snowfall amounts range from about 100 mm snow water equivalent (swe) on average in the Canadian Prairies to 400 mm swe on average in northern Québec. Onset of the snowcover begins on average by early October in the northern sections of the basin and progresses southward until on average mid-November when all of the HJUBs basin is snow-covered (McKay and Gray 1981). Snowmelt begins in the Canadian Prairies on average by mid-April but does not start until mid-June on average in northern Québec and Nunavut. Continuous and discontinuous permafrost is common at latitudes above

51°N (Woo 1986). Vegetation progresses from prairie grasslands in the headwaters of the Nelson River to the boreal forest across most of HJUBs, and then Arctic tundra in Nunavut and northern Québec.

3. Dataset and Methods

Freshwater discharge rates for rivers that drain into HJUBs are compiled in Environment Canada’s Hydrometric Database (HYDAT; Environment Canada 1994, 2004b). HYDAT is a comprehensive observational database that provides daily discharge rates (in $\text{m}^3 \text{s}^{-1}$) for most of the main rivers that flow into HJUBs. At least partial data exist for the 42 rivers listed in Table 1. Additional information on the maximum area over which gauge data are available for each river basin and the geographical coordinates of these recording stations are found in Table 1. The total maximum area that is monitored equals 80% of the overall territory covered by the HJUBs drainage basin. Temporal coverage between 1964 and 2000 is good for the largest rivers; however, smaller streams and rivers are generally not well sampled. Therefore, the following steps are adopted to provide complete temporal coverage of freshwater discharge for the rivers of interest.

Flow rates recorded by the gauge nearest to the rivers’ outlet into HJUBs are first used as the most representative for the entire basin. In situations where there are missing data, measurements from an upstream recording gauge along the river are used if available. In these instances, the river runoff rates are adjusted to reflect the missing contributing area to total discharge such that:

$$R_d = R_u A_d / A_u, \quad (1)$$

where R ($\text{m}^3 \text{s}^{-1}$) denotes the runoff rate over an area A (m^2) and where the subscripts u and d identify the upstream and downstream locations. Table 3 provides a comparison of daily river discharge for the Petite Rivière de la Baleine as measured by a gauge at 55.73°N , 74.69°W and the daily reconstructed river discharge for the same location based on gauge measurements recorded concurrently upstream at 55.68°N , 74.33°W . The error analysis in Table 3 demonstrates that the reconstructed runoff rates match the observations well for the period 1974-1989.

In some instances, discharge rates are completely unavailable for certain rivers throughout the period 1964-2000. To fill these gaps in the dataset, an additional procedure is followed. The annual cycle of daily discharge rates for each river is first constructed based on all of the available data for the period 1964-2000. Time series of daily discharge rates are then compiled from all of the available gauge measurements. During the construction of these time series, however, flow rates may be missing for a given river. In that case, discharge rates are estimated from the mean daily value for that river over 1964-2000. However, the streamflow rates for the missing site are adjusted according to the deviation in discharge from the mean of all rivers for which data are available on that specific day. For example, let us assume that the mean runoff for three separate rivers on a given day is \overline{R}_1 , \overline{R}_2 , and \overline{R}_3 , respectively. In constructing the time series of river discharge for that day (elements R_1 , R_2 , and R_3), a missing value may be encountered for station 3. In that instance, the river discharge for that site is estimated from:

$$R_3 = \frac{R_1 + R_2}{\overline{R}_1 + \overline{R}_2} \times \overline{R}_3. \quad (2)$$

The accuracy of this methodology over a period of 15 years is demonstrated in Table

3 for the Petite Rivière de la Baleine (55.73°N, 74.69°W). All of the available discharge data for the Petite Rivière de la Baleine were eliminated from the database and then reconstructed using the above method. Although the reconstructed discharge data are not as accurate as those based on an upstream gauge, they provide reasonable data that ensure continuous time series in each of the 42 rivers of interest.

In the presentation of our results, we choose not to remove the anthropogenic impact on river discharge. Indeed, seven of the major rivers that drain into HJUBs are impacted by dams, diversions, and/or reservoirs (Table 4). Major dams exist on the La Grande, Moose, and Nelson Rivers, whereas part of the Koksoak, Churchill, Eastmain, and Opinaca Rivers have been partially diverted to feed other rivers for enhanced hydroelectric power generation (Prinsenber 1980; Messier et al. 1986). Although dams were constructed prior to 1964 on the Nelson and Moose Rivers, other rivers did not incur similar anthropogenic influences until about 1980. At this time, the Eastmain, Opinaca, and Koksoak Rivers were all partly diverted from their natural courses to create large reservoirs that now feed La Grande Rivière where the massive James Bay hydroelectric complex was constructed by Hydro-Québec (Messier et al. 1986). Part of the Churchill River was diverted in 1976/77 to enhance the discharge of the Nelson River where Manitoba Hydro operates four large power generating plants (Prinsenber 1980).

Discharge data near the mouths of La Grande Rivière, the Opinaca River, and the Eastmain River are unavailable after 1980 in the HYDAT dataset. Therefore, the streamflow computed for these three rivers is based on measurements taken upstream from dams and/or river diversions. Discharge for the Opinaca and Eastmain Rivers after 1980 is therefore overestimated since this water is nearly all diverted into La Grande Rivière system (Messier et al. 1986). Nevertheless, we expect the total

estimates for the three rivers to correspond well with the artificially enhanced flow of La Grande Rivière. To test this hypothesis, we obtained a dataset of monthly discharge rates valid for the mouth of La Grande Rivière carried out by Hydro-Québec (R. Roy 2003, personal communication). Figure 2 presents a comparison of the monthly discharge rates for this system based on the Hydro-Québec data that are compared to the sum of the monthly discharge rates for the La Grande, Opinaca, and Eastmain Rivers inferred from the HYDAT data over 1981-94. It shows a good correspondence ($r^2 = 0.87$) between the two datasets, with HYDAT yielding only 2% more runoff than the Hydro-Québec dataset. This suggests that the total flow of La Grande Rivière, Opinaca River, and Eastmain River as determined from the HYDAT dataset remains accurate even after 1980. In this study, we maintain separate values for the flow of the La Grande, Eastmain, and Opinaca Rivers with the understanding that after 1980, their total is representative of the artificially enhanced discharge in La Grande Rivière. However, care is required in interpreting trends in these three rivers after 1980.

We choose not to remove the anthropogenic effects on HJUBs river discharge since we are interested in examining the actual amounts of freshwater entering high-latitude oceans. The investigation in section 6 of trends in upper ocean salinity measurements from the inner Newfoundland Shelf requires observed HJUBs river discharge that include anthropogenic effects. Nonetheless, it is important to distinguish natural trends from those imposed by human activity. Thus where possible, we compare trends in observed river discharge between naturally flowing and artificially influenced systems.

For the investigation of trends in freshwater discharge into HJUBs, we define a normalized runoff anomaly (NRA) as (Myers et al. 1990):

$$\text{NRA} = \frac{R_i - \bar{R}}{\sigma_R} \quad (3)$$

where the subscript i denotes the runoff for an individual year, the overbar denotes the annual average value for the period 1964-2000, and σ_R denotes the standard deviation of R . Positive (negative) values of the NRA indicate above (below) average discharge rates for a given river. This quantity allows direct comparisons of streamflow anomalies despite their wide range in absolute values. The method by which trends and their significance are established is given in the Appendix.

4. Results

a. Daily and annual characteristics of river discharge into HJUBs

The annual total mean discharge for each of the 42 rivers is presented in Table 5. This shows that the Nelson River, the basin with the largest area, provides 94.2 km³ of freshwater annually to Hudson Bay for the period 1964-2000. Other rivers that contribute a significant amount of freshwater are La Grande Rivière, the Koksoak River, Chesterfield Inlet, and the Moose River. Note that the combined river discharge of the La Grande, Opinaca, and Eastmain Rivers totals 100.0 km³ yr⁻¹. As a result of river diversions, the artificially enhanced discharge of La Grande Rivière surpasses that of the Nelson River after 1980. The total for the 42 rivers amounts to 714 km³ yr⁻¹, a rate equivalent to 0.023 Sv.

To obtain the contribution of river discharge to the surface water budget of each basin, we divide the yearly streamflow rates by the watershed's area. Table 5 shows that the runoff rates of 71 and 84 mm yr⁻¹ for the Churchill and Nelson Rivers are the lowest of all 42 rivers of interest. Relatively low precipitation and high

evaporation/sublimation rates in the Canadian Prairies (e.g., Déry and Yau 2002; Serreze et al. 2003) combined with the elevated retention rates of Lake Winnipeg and other reservoirs produce a low yield for these rivers. This is in contrast to the rivers along the eastern shore of Hudson and James Bays where an annual yield of up to 752 mm yr^{-1} in Chenal Goulet is found. Figure 3 presents the annual yield for each of the 42 rivers, beginning with the northwesternmost river (the Kirchoffer River on Southampton Island), moving southeastward along the perimeter of HJUBs to the easternmost location, the George River in Québec. This illustrates the relatively low yield ($\approx 200 \text{ mm yr}^{-1}$) of the rivers in Nunavut, a minimum for the rivers of Manitoba, and increasing contributions from west to east in the rivers of Ontario. The maximum annual yields are found on the eastern shores of James and Hudson Bays in the province of Québec, with slightly decreasing values in those rivers discharging into Ungava Bay.

Table 6 partitions the contributions of each province to the total discharge into HJUBs. Québec provides greater than half of the total freshwater discharge into HJUBs, with nearly equal contributions from Ontario and Manitoba (20% and 18%, respectively), and the remaining 10% having Nunavut as its source. James Bay collects slightly less freshwater than Hudson Bay despite its much smaller contributing area. Ungava Bay receives 19% of the total freshwater discharged into the system.

Figure 4 presents the annual cycle of river discharge into HJUBs. Flow rates are relatively low during winter and early spring, achieving a minimum of $0.68 \text{ km}^3 \text{ day}^{-1}$ on average in late March. As spring advances, snowmelt accelerates the rate of discharge and the mean annual maximum flow rate of $4.2 \text{ km}^3 \text{ day}^{-1}$, as a whole, is reached on average in mid-June. During summer and early fall, river discharge remains relatively high, with a secondary maximum of $2.3 \text{ km}^3 \text{ day}^{-1}$ attained on

average during the first week of October. Discharge rates then gradually decrease to the low flow regime of the winter season.

The individual contributions of each river to the total daily freshwater discharge rates are illustrated in Fig. 5. This shows that the Nelson River dominates the late fall and winter flow regimes, contributing up to 34% of the overall daily discharge by late March. Another important river is the La Grande that adds up to another 12% of the total daily runoff during the cold season. During April, the southernmost rivers, such as the Albany and the Moose, rapidly expand their relative contributions (up to 35% combined in late April) to total daily discharge in response to snowmelt. As melt progresses northward, rivers such as the Koksoak and Chesterfield Inlet begin to dominate whereas the contribution of more southern systems diminishes. Smaller rivers add little, if any, discharge during the cold season but incur significant peaks during snowmelt and supply considerable summertime runoff. This regime is more typical of the northernmost rivers such as those in Nunavut (e.g., the Lorillard and the Tha-anne) or in northern Québec (e.g., the Arnaud and the aux Feuilles).

b. Trends in river discharge into HJUBs

Figure 6 depicts the trend in the total annual discharge rates recorded for 42 rivers with outlets into HJUBs. Significant interannual variability exists in total discharge rates, with a range of $310 \text{ km}^3 \text{ yr}^{-1}$ between the annual maximum ($863 \text{ km}^3 \text{ yr}^{-1}$ in 1966) and minimum ($553 \text{ km}^3 \text{ yr}^{-1}$ in 1989) runoff rates. Interannual variability explains deviations of up to $\pm 22\%$ from the mean annual runoff rates. According to the Kendall-Theil Robust Line (see the Appendix), the overall trend shows a significant decrease ($-2.6 \text{ km}^3 \text{ yr}^{-1} \text{ yr}^{-1}$) in the amount of freshwater reaching the HJUBs over 1964-2000 at the $p < 0.05$ level. For this system alone, it

represents a reduction of $96 \text{ km}^3 \text{ yr}^{-1}$, equivalent to 0.003 Sv , over a period of 37 years.

Figure 7 provides the annual normalized runoff anomalies for the 42 rivers of interest over the period 1964-2000. Included in each panel of this plot are the Kendall-Theil Robust Lines depicting either increasing river discharge in black or decreasing river discharge in red. Over the 37-year period, 36 out of the 42 rivers show decreasing discharge into HJUBs between 1964-2000, with 21 rivers not affected by human impacts exhibiting negative trends that are significant at the $p < 0.05$ level.

Large and significant declines in freshwater discharge in the Churchill and Koksoak Rivers are attributed to their partial diversions into the Nelson and La Grande Rivière systems, respectively (Fig. 7 and Table 4). To investigate the natural variability in the basins affected by river diversions, we constructed two additional time series of normalized runoff anomalies representing the combined flow of 1) the Churchill and Nelson Rivers and 2) the La Grande, Koksoak, Eastmain, and Opinaca Rivers (not shown). Analysis of these two time series using the Mann-Kendall test shows that both systems exhibit negative but insignificant trends in observed discharge between 1964-2000. This suggests that the diversion of other rivers into the Nelson and La Grande Rivière systems induces, at least partially, the positive trends in their observed river discharge. Figure 7 therefore reveals a coherent, regional decline in the natural flow of HJUBs river discharge between 1964 and 2000.

The gradual reduction in freshwater discharge into HJUBs is also evident in the annual cycle of daily runoff rates for four selected time frames (Fig. 8). The

results illustrate a trend toward a decrease in summer and early fall runoff, but little change during winter and spring. There is a marked decrease in peak flow ($\approx 1 \text{ km}^3 \text{ day}^{-1}$) from 1964-76 to 1988-2000. The “flattening” of the annual maximum over time suggests increasing flow control and water retention by upstream dams and reservoirs (Anctil and Couture 1994; McClelland et al. 2004). It is also interesting to note that the secondary maximum in river discharge during fall nearly vanishes between 1976-1988 but reappears in 1988-2000 with greater amplitude and at an earlier stage than in 1964-76.

c. Role of snowcover

Snow covers the surface of the HJUBs from 130 to 240 days each year (McKay and Gray 1981). As a result of its accumulation during the cold season, spring runoff is dominated by meltwater that yields an annual peak in total discharge within the HJUBs. Table 6 includes the mean peak flow rates observed each spring and the mean date at which this event occurs. The largest streamflow rates attain $10275 \text{ m}^3 \text{ s}^{-1}$ on average each spring transition period in the Koksoak, demonstrating the critical role played by snow in the hydrology of high-latitude watersheds. The earliest peak discharge rates occur during the first week of May in several James Bay rivers, whereas the latest peak discharge rates are observed in the Povungnituk (on average in early July). For the system as a whole, maximum flow rates of nearly 0.05 Sv per day occur in mid-June.

Figure 9 shows there is a good correspondence ($r^2 = 0.71$) between the latitude of the outlets for each of the 42 rivers and the day at which runoff attains its mean annual peak. The linear regression based on these data yields:

$$\text{JD} = 4.9\phi - 120 \quad (4)$$

where ϕ is latitude (degrees north) and where JD represents the julian day of the observed peak in river runoff. The slope in Eq. (4) suggests that there is a difference of 5 days in the occurrence of peak discharge rates associated with snowmelt for each degree of latitude. Thus snowmelt induces peak discharges rates on average in early May at 50°N but not until late June at 60°N . Owing to its wide range of latitudes, the HJUBs undergo snowmelt for a period of at least two months (mostly in May and June) of each year.

Figure 10a represents the mean departure (in days) from the mean annual date at which the spring peak discharge rates are observed in the HJUBs. Although there is significant variability in the timing of the freshet (± 16 days), there is an overall trend toward an earlier snowmelt. The trend analysis shown in Fig. 10 reveals that the onset of melt has advanced on average by eight days between 1964 and 2000. A similar trend analysis excluding the seven rivers affected by dams, diversions, and reservoirs yields an advance of only four days in the timing of spring peak discharge rates. Figure 10b illustrates that the intensity of the observed peak discharge rates during spring has diminished by $420 \text{ m}^3 \text{ s}^{-1}$ over the 37 years of interest. Similar to the date of snowmelt, there is considerable interannual variability in the flow rates recorded during spring, with anomalies ranging from -400 to $700 \text{ m}^3 \text{ s}^{-1}$. Despite the decreasing trend in this quantity, the largest positive anomalies occurred during the second half of the study period (i.e. 1979, 1985, 1986, and 1992). For the 35 rivers not affected by human impacts, the observed spring peak discharge rates has decreased on average by $302 \text{ m}^3 \text{ s}^{-1}$. As illustrated in Fig. 8, the regulation of water has a tendency to diminish the intensity and alter the timing of the spring freshets

(Anctil and Couture 1994; McClelland et al. 2004).

5. Comparison with Other Studies

A comparison of the mean annual discharge rates obtained in this study with the values compiled by the Natural Resources Canada (2004) in the *Atlas of Canada* for 22 of the largest rivers that drain into HJUBs is shown in Fig. 11. There is good agreement ($r^2 = 0.85$) between the two datasets. Discrepancies may arise at selected time periods (time periods are not specified in the *Atlas of Canada*). To compare the total annual discharge rates into Hudson Bay and Hudson Strait, we adjust our results to include the missing 20% in contributing area to our calculations. The adjusted total discharge rate of $888 \text{ km}^3 \text{ yr}^{-1}$ for the HJUBs drainage system compares well with the $938 \text{ km}^3 \text{ yr}^{-1}$ reported by Shiklomanov and Shiklomanov (2003) for the period 1966-99.

Trends in Canadian streamflow have recently been assessed by Zhang et al. (2001). The authors employed river runoff data from 243 stations that are part of the Reference Hydrometric Basin Network (RHBN; Harvey et al. 1999) across Canada with temporal coverage beginning in 1947. For the period 1967-96, the authors find a significant upward trend in the discharge into Chesterfield Inlet whereas other rivers in northern Ontario and Québec show declining streamflow rates. This pattern is consistent with the results of Whitfield and Cannon (2000) who used cluster analysis to inspect trends in streamflow between 1976 and 1995 for 650 river basins of Canada. Furthermore, Ingram et al. (1996) reported a diminishing trend in the runoff of the Grande Rivière de la Baleine in northern Québec between 1962 and 1991. These studies are in general agreement with the trend analysis carried here for the 42 rivers draining into HJUBs over the period 1964-2000. Peterson et al.

(2002) report a 7% increase in Siberian river discharge between 1936 and 1999. This equates to an additional input of $128 \text{ km}^3 \text{ yr}^{-1}$ of freshwater to the Arctic Ocean by the end of their study period. In Hudson Bay and Hudson Strait, an opposite trend is observed, with a decline of $96 \text{ km}^3 \text{ yr}^{-1}$ or of 13% in freshwater discharge by 2000. Further analysis of the normalized runoff anomalies in HJUBs between 1964-89 reveals a decrease of $148 \text{ km}^3 \text{ yr}^{-1}$ (significant at the $p < 0.01$ level) that balances the overall change observed in Siberia.

6. Discussion

River discharge into high-latitude oceans affects the salinity and the stability of the upper ocean, and hence sea ice formation and the global thermohaline circulation (Aagaard and Carmack 1989; Manak and Mysak 1989). Sutcliffe et al. (1983) proposed a link between freshwater discharge into Ungava Bay and upper ocean salinity anomalies observed four months later on the Newfoundland Shelf in the Northwestern Atlantic Ocean. Myers et al. (1990) investigated this link in greater detail and established a negative correlation between enhanced Hudson Bay and James Bay river discharge and the upper ocean salinity observed nine months later at Station 27, an oceanographic station located at 47.5°N , 52.6°W on the inner Newfoundland Shelf.

To explore further the findings of Sutcliffe et al. (1983) and Myers et al. (1990), a dataset of ocean salinity covering the period 1964-94 has been acquired from the Canadian Marine Environmental Data Services (MEDS). Salinity measurements taken within the upper layer ($< 50 \text{ m}$) of the ocean for a 25 km^2 grid box that encompasses Station 27 are extracted from the MEDS archive. An algorithm that follows the approximate path taken by HJUBs freshwater into Hudson Bay, Hudson

Strait, and then out into the Labrador Current is also developed. We compute the mean distance between the outlet of each river to points along the dominant wind-driven currents in the area. In Hudson Bay, the surface currents form a cyclonic gyre with a mean current speed of $\sim 0.04 \text{ m s}^{-1}$ (Prinsenber 1980, 1986a). Arriving in Hudson Strait, the water accelerates along the Québec coastline at a speed of $\sim 0.15 \text{ m s}^{-1}$ (Prinsenber 1986b; Drinkwater 1986), and then deflects southward into the Labrador Current where the water travels along the Labrador and Newfoundland shelves at about 0.5 m s^{-1} (Reynaud et al. 1995; LeBlond et al. 1981; 1996). The tracking algorithm follows the spring/summer pulse of freshwater that arises from continental snowmelt with realistic contributions and delays for each of the 42 rivers that drain into HJUBs. This methodology serves as a useful diagnostic tool to estimate the timing and intensity of downstream freshwater pulses and salinity anomalies in the top layers of the ocean.

Figure 12 provides the contributions of four selected regions along the perimeter of HJUBs to the pulse of freshwater inferred for Station 27 between 1970 and 1972. The time period is restricted here to three years to improve clarity of the results. It shows a phasing of the peaks in river runoff from three sections along the perimeter of the drainage system: Ungava Bay, James Bay, and Western Hudson Bay. Discharge from Ungava Bay exhibits the strongest seasonal cycle and leads to the sudden peaks in the freshwater pulses. The seasonal cycle of river discharge into James Bay and Western Hudson Bay is not as pronounced but still displays a significant peak arising from snowmelt that is in phase (with a lag of one and two years, respectively) with that of Ungava Bay. Table 7 lists the 42 rivers of interest in order along the perimeter of Western Hudson Bay, James Bay, Eastern Hudson Bay, and Ungava Bay, the approximate number of days that water from the river outlets takes to

reach Station 27 on the inner Newfoundland Shelf, and the distance traveled over that time. The table also includes the julian day at which a crest in river discharge induced by snowmelt reaches this ocean location. Of interest is the phasing of the contributions from Western Hudson Bay (with more than a two year delay), James Bay (with more than a one year delay), and Ungava Bay (with a three month delay) to the freshwater pulse arriving at Station 27 during summer. As many as 22 rivers with outlets into HJUBs see their meltwater peaks reach Station 27 on average between 1 July and 31 September.

Figure 13 depicts the upper ocean salinity observed at Station 27 between 1966 and 1994 in addition to the pulse of freshwater that arises from river runoff into HJUBs as computed by the tracking algorithm for this location. Freshwater pulses for 1964 and 1965 are omitted owing to the 2-year delay required for some of the water to reach Station 27. There is a strong annual peak in the pulse of freshwater that resembles high discharge rates associated with snowmelt. Peak transport values typically reach 0.05 Sv each year during summer; the peaks correspond well with the annual minima in upper ocean salinity observed at Station 27. This supports the results of Sutcliffe et al. (1983) and Myers et al. (1990) that suggest a negative correlation between continental runoff into HJUBs and ocean salinity of the inner Newfoundland Shelf. However, the tracking algorithm suggests that the freshwater pulses are composed of meltwater from three successive winter seasons rather than a single one as proposed by Sutcliffe et al. (1983) and Myers et al. (1990).

Figure 14 presents the magnitude of the annual freshwater pulse between 1 July and 31 September and the corresponding upper ocean salinity values. Accompanying the diminishing discharge rates into HJUBs between 1966-94 are increasing upper ocean salinity values on the inner Newfoundland Shelf. Over the 29-year period,

the summertime freshwater pulse has declined by 0.003 Sv and has resulted in an upper ocean that is 0.2 parts per mil more saline at Station 27. The analysis presented in this section implies that interannual to decadal variations and trends in precipitation, snowcover, and river runoff over North America may play a key role in governing the state of the upper layers of the Arctic Ocean and Northwestern Atlantic Ocean.

Despite its simplicity, the methodology used here to track freshwater pulses has limitations. It assumes no dispersion of the freshwater along a trajectory and does not consider tidal mixing, precipitation, or ice melt that exert a significant control on the upper layers of the ocean in the Labrador Current (Prinsenberg 1984; Mertz et al. 1993; Myers et al. 1993). In other words, we assume the freshwater discharge to be a passive tracer in the analysis. A more comprehensive approach will require the use of coupled atmosphere/ocean/sea ice/land surface models to better track the evolution and impact of freshwater discharge from HJUBs to the Labrador Current and at downstream locations. In future work, we will therefore conduct simulations with a global climate model to establish the precise role of the HJUBs' freshwater discharge on the state of the Arctic and Atlantic Oceans and its contribution to the global thermohaline circulation.

7. Summary and Future Work

We examined the characteristics and trends of observed river discharge into Hudson, James, and Ungava Bays for the period 1964-2000. Forty-two rivers with outlets into these bays contribute on average $714 \text{ km}^3 \text{ yr}^{-1}$ ($=0.023 \text{ Sv}$) of freshwater to high-latitude oceans. For the system as a whole, discharge attains an annual peak of $4.2 \text{ km}^3 \text{ day}^{-1}$ on average in mid-June, whereas the minimum of $0.68 \text{ km}^3 \text{ day}^{-1}$

occurs on average in the first week of April. The Nelson River contributes as much as 34% of the daily discharge for the entire system during winter, but diminishes in relative importance during spring and summer. Runoff rates per contributing area are highest (lowest) on the eastern (western) shores of Hudson and James Bays. Linear trend analyses reveal decreasing discharge over the 37-year period in 36 out of the 42 rivers, 33 of which are not affected by dams, diversions, and/or reservoirs. By 2000, the total annual freshwater discharge into the Arctic Ocean diminished by 96 km^3 from its value in 1964, equivalent to a reduction of 0.003 Sv. The annual spring peak discharge rates associated with snowmelt has advanced by nine days between 1964 and 2000 and has diminished by $0.036 \text{ km}^3 \text{ day}^{-1}$ in intensity. There is a direct correlation between the timing of peak spring discharge rates and the latitude of a river's mouth; the spring freshet varies by five days for each degree of latitude. Continental snowmelt induces a seasonal pulse of freshwater from HJUBs that is tracked along its path into the Labrador Current. It is suggested that the annual upper ocean salinity minimum observed at Station 27 on the inner Newfoundland Shelf can be explained by freshwater pulses composed of meltwater from three successive winter seasons in the river basins draining into HJUBs. A gradual salinization of the upper ocean during summer over the period 1966-94 at Station 27 is in accord with a decadal trend of a diminishing intensity in the continental meltwater pulses.

A recent study by Déry and Wood (2004) documents a strong anticorrelation between the Arctic Oscillation (AO; Thompson and Wallace 1998) and HJUBs river discharge. Déry and Wood (2004) suggest that the climatological sea-level pressure patterns during the alternating phases of the AO influence the dominant air masses affecting the basin. During the positive (negative) polarity of the AO, relatively

cool, dry (warm, wet) air masses impact the eastern half of the HJUBs leading to substantial decreases (increases) in overall basin discharge. The recent trend toward the positive phase of the AO has cooled air temperatures and diminished precipitation in the eastern half of HJUBs (e.g., Serreze et al. 2000). This suggests that the observed decrease in HJUBs river discharge is driven by large-scale atmospheric anomalies such as the AO. A comprehensive water budget of the HJUBs has been initiated to explore in detail the link between the AO and river discharge and will be reported in a future study.

Acknowledgments

We thank R. Roy (Ouranos in Montréal) who generously provided La Grande Rivière discharge data collected by Hydro-Québec, D. Spear (Canadian Marine Environmental Data Services in Ottawa) who kindly supplied the ocean salinity data for the inner Newfoundland Shelf, and J. Sheffield (Princeton University) for support in the trend analyses. Insightful comments by R. Brown (CMC Dorval), N. Roulet (McGill University) and one anonymous referee are also gratefully acknowledged. This project has been funded through support from grant NSF OPP02-30211 (Collaborative research: The role of spatial and temporal variability of Pan-Arctic river discharge and surface hydrological processes on climate to E. F. Wood). We acknowledge that funding for M. Stieglitz is provided from NSF grants from the Office of Polar Programs (OPP-002369), from the division of Environmental Biology (Arctic LTER Project), and from an NSF Cooperative Agreement (OPP-0002239), as well as the NASA Seasonal-to-Interannual Prediction Project at Goddard Space Flight Center, NASA's Global Modeling and Analysis Program under RTOP 622-24-47, and the NSF Biocomplexity award ATM 0221835. This report was prepared by S. J. Déry under award NA17RJ2612 from National Oceanic and Atmospheric

Administration (NOAA), U.S. Department of Commerce. The statements, findings, conclusions, and recommendations are those of the author and do not necessarily reflect the views of NOAA or the U.S. Department of Commerce.

APPENDIX

Detection and Significance of Trends in River Discharge

From the time series of NRA values, the magnitude of the trends in river discharge are established using the Mann-Kendall test (Mann 1945; Kendall 1975). This statistical test has been used in several other studies to detect changing hydrological regimes (e.g., Lettenmaier et al. 1994; Ziegler et al. 2003). The Kendall-Theil Robust Line (Theil 1950) develops a linear equation from a time series of n -elements such as:

$$y = mt + b \tag{A1}$$

where t is time (year) and y denotes river runoff. To determine the slope m of Eq. (A1), the slopes m_k for each tied group of river discharge data are computed as:

$$m_k = \frac{(y_j - y_i)}{(t_j - t_i)} \tag{A2}$$

where $k = 1, 2, \dots, n(n-1)/2$, $i = 1, 2, \dots, n-1$, and $j = 2, 3, \dots, n$. The median slope of all elements m_k is then taken as the slope of Eq. (A1). The coefficient b is obtained by substituting the median time and river discharge values in Eq. (A1) and solving for b . This provides the Kendall-Theil Robust Line for each time series of river discharge as well as the magnitude of this trend (m).

Since river discharge is not well represented by the standard normal distribution (Lettenmaier et al. 1994), we follow these steps to establish the significance of the

river discharge trends: First, a test statistic S is defined as:

$$S = \sum_{k=1}^{n(n-1)/2} \text{sgn}(m_k) \quad (\text{A3})$$

where sgn is the sign function and equals 1, 0, or -1 for positive, zero, or negative values of m_k , respectively. For the null hypothesis and in the absence of ties, σ_S , the variance of S , is given by

$$\sigma_S = \frac{n(n-1)(2n+5)}{18}. \quad (\text{A4})$$

Then to obtain a test statistic that is closely approximated by the standard normal distribution, Z_s is specified as (Ziegler et al. 2003):

$$Z_s = \begin{cases} \frac{(S-1)}{\sigma_S} & S > 0 \\ 0 & S = 0 \\ \frac{(S+1)}{\sigma_S} & S < 0 \end{cases} \quad (\text{A5})$$

From this distribution, the significance of a trend at a level p is established if $|Z_s| > p(f)$, where f is the standard normal distribution. From these steps, trends of river discharge are assigned a magnitude and a significance level.

References

- Aagaard, K., and E. C. Carmack, 1989: The role of sea ice and other freshwater in the Arctic circulation. *J. Geophys. Res.*, **94**(C10), 14 485-14 498.
- Anctil, F., and R. Couture, 1994: Impacts cumulatifs du développement hydro-électrique sur le bilan d'eau douce de la baie d'Hudson. *Can. J. Civil Eng.*, **21**(2), 297-306.
- Anderson, L. G., S. Jutterström, S. Kaltin, E. P. Jones, and G. Björk, 2004: Variability in river runoff distribution in the Eurasian Basin of the Arctic Ocean. *J. Geophys. Res.*, **109**, C01016, doi: 10.1029/2003JC001773.
- Brown, R. D., and R. O. Braaten, 1998: Spatial and temporal variability of Canadian monthly snow depths. *Atmos.-Ocean*, **36**, 37-54.
- Carmack, E. C., 2000: The Arctic Ocean's freshwater budget: sources, storage and export. *The Freshwater Budget of the Arctic Ocean*, E. L. Lewis et al., Eds., Nato Science Series, 2. Environmental Security Vol. 7, Kluwer Academic Publishers, 91-126.
- Chapman, W. L., and J. E. Walsh, 1993: Recent variations in sea ice and air temperature in high latitudes. *Bull. Amer. Meteor. Soc.*, **74**, 33-47.
- Curtis J., G. Wendler G, R. Stone, and E. Dutton, 1998: Precipitation decrease in the western Arctic, with special emphasis on Barrow and Barter Island, Alaska. *Int. J. Climatol.*, **18**, 1687-1707.
- Déry, S. J., and E. F. Wood, 2004: Teleconnection between the Arctic Oscillation and Hudson Bay river discharge. *Geophys. Res. Lett.*, **31**(18), L18205, doi: 10.1029/2004GL020729.
- Déry, S. J., and M. K. Yau, 2002: Large-scale mass balance effects of blowing snow and surface sublimation. *J. Geophys. Res.*, **107**, 4679, doi: 10.1029/2001JD001251.
- Drinkwater, K. F., 1986: Physical oceanography of Hudson Strait and Ungava Bay. *Canadian Inland Seas*, I. P. Martini, Ed., Elsevier, 237-264.
- Environment Canada, 1994: *HYDAT CD-ROM Version 4.93*. Surface Water and Sediment Data, Atmospheric Environment Service, Water Survey of Canada.
- Environment Canada, 2004a: *Canadian Climate Normals 1971-2000*. Canadian Climate and Water Information, available online at: <http://www.climate.weatheroffice.ec.gc.ca/>

climate_normals/index_e.html.

- Environment Canada, 2004b: *Archived Hydrometric Data (HYDAT)*. Water Survey of Canada, available online at: http://www.msc.ec.gc.ca/wsc/hydat/H2O/index_e.cfm.
- Gagnon, A. S., and W. A. Gough, 2004: Climate change scenarios for the Hudson Bay region: An intermodel comparison. *Climatic Change*, in press.
- Gough, W. A., and E. Wolfe, 2001: Climate change scenarios for Hudson Bay, Canada, from general circulation models. *Arctic*, **54**, 142-148.
- Harvey, K. D., P. J. Pilon, and T. R. Yuzyk, 1999: Canada's reference hydrometric basin network (RHBN): In partnerships in water resource management. Paper presented at CWRA 51th Annual Conference, Can. Water Resour. Assoc., Halifax, Nova Scotia.
- Ingram, R. G., J. Wang, C. Lin, L. Legendre, and L. Fortier, 1996: Impact of freshwater on a subarctic coastal ecosystem under seasonal sea ice (southeastern Hudson Bay, Canada). I. Interannual variability and predicted global warming influence on river plume dynamics and sea ice. *J. Mar. Syst.*, **7**, 221-231.
- Kendall, M. G., 1975: *Rank Correlation Methods*. Charles Griffin, 202 pp.
- Lammers, R. B., A. I. Shiklomanov, C. J. Vörösmarty, B. M. Fekete, and B. J. Peterson, 2001: Assessment of contemporary Arctic river runoff based on observational discharge records. *J. Geophys. Res.*, **106**(D4), 3321-3334.
- LeBlond, P. H., T. F. Osborn, D. O. Hodgins, R. Goodman, and M. Metge, 1981: Surface circulation in the western Labrador Sea. *Deep-Sea Res.*, **28**, 683-693.
- LeBlond, P. H., J. R. Lazier, and A. J. Weaver, 1996: Can regulation of freshwater runoff in Hudson Bay affect the climate of the North Atlantic? *Arctic*, **49**(4), 348-356.
- Lettenmaier, D. P., E. F. Wood, and J. R. Wallis, 1994: Hydro-climatological trends in the continental United States, 1948-1988. *J. Climate*, **7**, 586-607.
- Manak, D. K., and L. A. Mysak, 1989: On the relationship between Arctic sea-ice anomalies and fluctuations in Northern Canadian air temperature and river discharge. *Atmos.-Ocean*, **27**(4), 682-691.
- Mann, H. B., 1945: Non-parametric test against trend. *Econometrika*, **13**, 245-259.

- McCabe, G. J., M. P. Clark, and M. C. Serreze, 2001: Trends in northern hemisphere surface cyclone frequency and intensity. *J. Climate*, **14**, 2763-2768.
- McClelland, J. W., R. M. Holmes, B. J. Peterson, and M. Stieglitz, 2004: Increasing river discharge in the Eurasian Arctic: Consideration of dams, permafrost thaw, and fires as agents of change. *J. Geophys. Res.*, **109**(D19), D18102, doi: 10.1029/2004JD004583.
- McKay, G. A., and D. M. Gray, 1981: The distribution of snowcover. *Handbook of Snow*, D. M. Gray and D. H. Male, Eds., Pergamon Press, 153-190.
- Mertz, G., S. Narayanan, and J. Helbig, 1993: The freshwater transport of the Labrador Current. *Atmos.-Ocean*, **31**(2), 281-295.
- Messier, D., R. G. Ingram, and D. Roy, 1986: Physical and biological modifications in response to La Grande hydroelectric complex. *Canadian Inland Seas*, I. P. Martini, Ed., Elsevier, 403-424.
- Myers, R. A., S. A. Akenhead, and K. Drinkwater, 1990: The influence of Hudson Bay runoff and ice-melt on the salinity of the inner Newfoundland Shelf. *Atmos.-Ocean*, **28**(2), 241-256.
- Myers, R. A., K. F. Drinkwater, N. J. Barrowman, and J. W. Baird, 1993: Salinity and recruitment of Atlantic cod (*Gadus morhua*) in the Newfoundland region. *Can. J. Fish. Aquat. Sci.*, **50**, 1599-1609.
- Natural Resources Canada, 2004: *Atlas of Canada*. Available online at: <http://atlas.gc.ca/>.
- Osterkamp, T. E., and V. E. Romanovsky, 1996: Characteristics of changing permafrost temperatures in the Alaskan Arctic, U.S.A. *Arct. Alp. Res.*, **28**, 267-273.
- Peterson, B. J., R. M. Holmes, J. W. McClelland, C. J. Vörösmarty, R. B. Lammers, A. I. Shiklomanov, I. A. Shiklomanov, and S. Rahmstorf, 2002: Increasing river discharge to the Arctic Ocean. *Science*, **298**, 2171-2173.
- Prinsenber, S. J., 1980: Man-made changes in freshwater input rates of Hudson and James Bays. *Can. J. Fish. Aquat. Sci.*, **37**, 1101-1110.
- Prinsenber, S. J., 1984: Freshwater contents and heat budgets of James Bay and Hudson Bay. *Cont. Shelf Res.*, **3**, 191-200.

- Prinsenber, S. J., 1986a: The circulation pattern and current structure of Hudson Bay. *Canadian Inland Seas*, I. P. Martini, Ed., Elsevier, 187-204.
- Prinsenber, S. J., 1986b: On the physical oceanography of Foxe Basin. *Canadian Inland Seas*, I. P. Martini, Ed., Elsevier, 217-236.
- Reynaud, T. H., A. J. Weaver, and R. J. Greatbatch, 1995: Summer mean circulation of the northwestern Atlantic Ocean. *J. Geophys. Res.*, **100**(C1), 779-816.
- Saucier, F., and J. Dionne, 1998: A 3-D coupled ice-ocean model applied to Hudson Bay, Canada: The seasonal cycle and time-dependent climate response to atmospheric forcing and runoff. *J. Geophys. Res.*, **103**(C12), 27 689-27 705.
- Saucier, F., S. Senneville, S. Prinsenber, F. Roy, G. Smith, P. Gachon, D. Caya, and R. Laprise, 2004: Modelling the sea ice-ocean seasonal cycle in Hudson Bay and Hudson Strait, Canada. *Climate Dyn.*, **23**, 303-326.
- Serreze, M. C., J. E. Walsh, F. S. Chapin III, T. Osterkamp, M. Dyrgerov, V. Romanovsky, W. C. Oechel, J. Morison, T. Zhang, and R. G. Barry, 2000: Observational evidence of recent change in the northern high-latitude environment. *Climatic Change*, **46**, 159-207.
- Serreze, M. C., D. H. Bromwich, M. P. Clark, A. J. Etringer, T. Zhang, and R. Lammers, 2003: Large-scale hydro-climatology of the terrestrial Arctic drainage system. *J. Geophys. Res.*, **108**(D2), 8160, doi:10.1029/2001JD000919.
- Shiklomanov, I. A., and A. I. Shiklomanov, 2003: Climatic change and the dynamics of river runoff into the Arctic Ocean. *Water Resour.*, **30**(6), 593-601, [translated from Russian].
- Shiklomanov, I. A., A. I. Shiklomanov, R. B. Lammers, B. J. Peterson, and C. J. Vorosmarty, 2000: The dynamics of river water inflow to the Arctic Ocean. *The Freshwater Budget of the Arctic Ocean*, E. L. Lewis et al., Eds., Nato Science Series, 2. Environmental Security Vol. 7, Kluwer Academic Publishers, 281-296.
- Shiklomanov, A. I., R. B. Lammers, and C. J. Vörösmarty, 2002: Widespread decline in hydrological monitoring threatens Pan-Arctic research. *Eos, Trans. Amer. Geophys.*

Union, **83**(2), 13.

- Stewart, R. E., H. G. Leighton, P. Marsh, G. W. K. Moore, W. R. Rouse, S. D. Soulis, G. S. Strong, R. W. Crawford, and B. Kochtubajda, 1998: The Mackenzie GEWEX Study: The water and energy cycles of a major North American river basin. *Bull. Amer. Meteor. Soc.*, **79**(12), 2665-2684.
- Stieglitz, M., S. J. Déry, V. E. Romanovsky, and T. E. Osterkamp, 2003: The role of snow cover in the warming of Arctic permafrost. *Geophys. Res. Lett.*, **30**(13), 1721, doi:10.1029/2003GL017337.
- Sutcliffe, W. J. Jr., R. H. Loucks, K. F. Drinkwater, and A. R. Coote, 1983: Nutrient flux onto the Labrador Shelf from Hudson Strait and its biological consequences. *Can. J. Fish. Aquat. Sci.*, **40**, 1692-1701.
- Theil, H., 1950: A rank-invariant method of linear and polynomial regression analysis. *Indagationes Math.*, **12**, 85-91.
- Thompson, D. W. J., and J. M. Wallace, 1998: The Arctic Oscillation signature in the wintertime geopotential height and temperature fields. *Geophys. Res. Lett.*, **25**, 1297-1300.
- Walsh, J. E., 2000: Global atmospheric circulation patterns and relationships to Arctic freshwater fluxes. *The Freshwater Budget of the Arctic Ocean*, E. L. Lewis et al., Eds., Nato Science Series, 2. Environmental Security Vol. 7, Kluwer Academic Publishers, 21-43.
- Weatherly, J. W., and J. E. Walsh, 1996: The effects of precipitation and river runoff in a coupled ice-ocean model of the Arctic. *Climate Dyn.*, **12**, 785-798.
- Whitfield, P. H., and A. J. Cannon, 2000: Recent variations in climate and hydrology in Canada. *Can. Water Resour. J.*, **25**(1), 19-65.
- Woo, M.-K., 1986: Permafrost hydrology in North America. *Atmos.-Ocean*, **24**(3), 201-234.
- Yang, D., D. L. Kane, L. D. Hinzman, X. Zhang, T. Zhang, and H. Ye, 2002: Siberian Lena River hydrologic regime and recent change. *J. Geophys. Res.*, **107**, doi:10.1029/2002JD002542.

- Zhang, X., K. D. Harvey, W. D. Hogg, and T. R. Yuzyk, 2001: Trends in Canadian streamflow. *Water Resour. Res.*, **37**(4), 987-998.
- Ziegler, A. D., J. Sheffield, E. P. Maurer, B. Nijssen, E. F. Wood, and D. P. Lettenmaier, 2003: Detection of intensification in global- and continental-scale hydrological cycles: Temporal scale of evaluation. *J. Climate*, **16**, 535-547.

Figure Captions

Figure 1: Geographical map of the Hudson Bay (HB) and James Bay (JB) drainage basin (gray shading) and of the Ungava Bay (UB) drainage basin (black shading).

Figure 2: Comparison of the monthly discharge rates for La Grande Rivière inferred from Hydro-Québec and from HYDAT, 1981-94. The solid line is the linear regression and the dashed line is the 1:1 line. The coefficient of determination (r^2), probability value (p), and standard error (s) of the linear regression are also given.

Figure 3: The mean annual discharge rates per contributing area for 42 rivers that drain into Hudson Bay (HB), James Bay (JB), and Ungava Bay (UB), 1964-2000. The order of the rivers along the perimeter of the drainage basin is given in Table 7. The province or territory where the mouths of the rivers are located is also provided. The following abbreviations are used: NU, Nunavut; MB, Manitoba; ON, Ontario; QC, Québec.

Figure 4: The annual cycle of freshwater discharge for 42 rivers that drain into Hudson, James, and Ungava Bays, 1964-2000.

Figure 5: The daily contribution (as a cumulative percentage) of 42 rivers to the freshwater discharge into Hudson, James, and Ungava Bays, 1964-2000.

Figure 6: The temporal evolution of the total annual freshwater discharge of 42 rivers that drain into Hudson, James, and Ungava Bays, 1964-2000. The thick solid line denotes the Kendall-Theil Robust Line.

Figure 7: The temporal evolution of the annual normalized runoff anomalies (NRA) for 42 rivers that drain into Hudson, James, and Ungava Bays, 1964-2000. The Kendall-Theil Robust lines are included as thick black (red) lines to indicate positive (negative) trends in freshwater discharge. Thick solid (dashed) lines denote rivers with (without) significant trends at the $p < 0.05$ level. Bold frames denote rivers affected by dams, diversions, and/or reservoirs.

Figure 8: The annual cycle of freshwater discharge for 42 rivers that drain into Hudson, James, and Ungava Bays, over four selected time periods.

Figure 9: The relationship between the date of maximum discharge rate versus the latitude for 42 rivers that drain into Hudson, James, and Ungava Bays, 1964-2000. The coefficient of determination (r^2), probability value (p), and standard error (s) of the linear regression (solid line) are also given.

Figure 10: The trend in a) the mean departure (in days) from the annual spring maximum discharge rates and in b) the annual spring peak discharge rate anomalies for 42 rivers that drain into Hudson, James, and Ungava Bays, 1964-2000. The thick black lines denote the Kendall-Theil Robust Lines.

Figure 11: Comparison of the annual discharge rates for 22 rivers that drain into Hudson, James, and Ungava Bays from the *Atlas of Canada* versus the results of this study. The solid line is the linear regression and the dashed is line the 1:1 line. The coefficient of determination (r^2), probability value (p), and standard error (s) of the linear regression are also given.

Figure 12: The instantaneous daily discharge rates for HJUBs as well as the contribution of four regions along the perimeter of Hudson Bay, James Bay, and

Ungava Bay to the total daily freshwater pulse inferred for Station 27 on the inner Newfoundland Shelf, 1970-72.

Figure 13: The daily freshwater pulse and upper ocean salinity values inferred for Station 27 on the inner Newfoundland Shelf, 1966-94.

Figure 14: The summertime freshwater pulse and upper ocean salinity values inferred for Station 27 on the inner Newfoundland Shelf, 1966-94. The thick black lines denote the Kendall-Theil Robust Lines.

Table Captions

Table 1: Alphabetical list of 42 rivers that discharge into Hudson Bay (HB), James Bay (JB), and Ungava Bay (UB), their outlet, province or territory, geographical coordinates of the recording gauge nearest to the mouth, and contributing area that is gauged. The following abbreviations are used: NU, Nunavut Territory; MB, Manitoba; ON, Ontario; QC, Québec.

Table 2: The mean annual conditions of air temperature (T), precipitation (P), and snowfall (S_f) at selected meteorological stations within the HJUBs drainage system for the period 1971-2000¹.

Table 3: Error analysis for the reconstructed (REC) river discharge compared to observations (OBS). The analysis is based on the mean daily values of river runoff between 18 June 1974 and 5 July 1988 for the Petite Rivière de la Baleine. Two reconstructions are presented: one based on upstream measurements (REC1) and the other based on the remaining available discharge data (REC2). The following abbreviations are used: r^2 , coefficient of determination; MAE, mean absolute error; RMSE, root mean square error.

Table 4: List of HJUBs rivers that are affected by major dams, diversions (div), and/or reservoirs (res) as well as the approximate year when major human impacts began.

Table 5: Annual discharge rates for 42 rivers that drain into Hudson, James, and Ungava Bays. The mean peak flow induced by meltwater and the julian day at which it occurs are also listed.

Table 6: Contribution of each bay and of each province or territory to the total freshwater discharge in Hudson, James, and Ungava Bays over the period 1964-2000.

Table 7: The delay (in days) it takes for freshwater discharge from 42 rivers along the perimeter of Hudson Bay, James Bay, and Ungava Bay, to reach Station 27 (47.5°N, 52.6°W) on the inner Newfoundland Shelf. The approximate distance between the mouth of the rivers to Station 27 and the julian day at which peak discharge rates associated with meltwater reaches this destination are also indicated. Bold values indicate peak freshwater pulses arriving at Station 27 on average between 1 July and 31 September of each year.

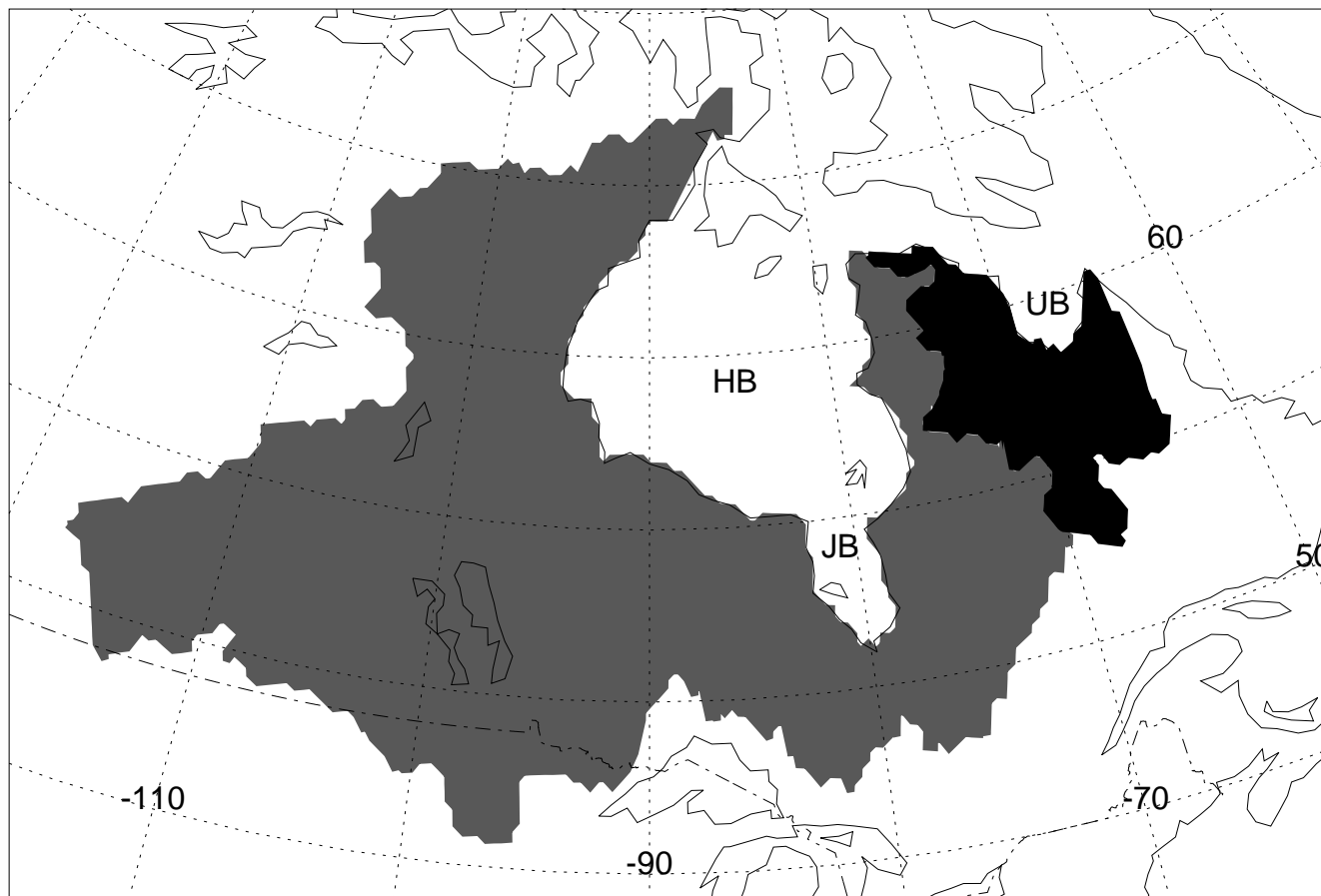


FIGURE 1: Geographical map of the Hudson Bay (HB) and James Bay (JB) drainage basin (gray shading) and of the Ungava Bay (UB) drainage basin (black shading).

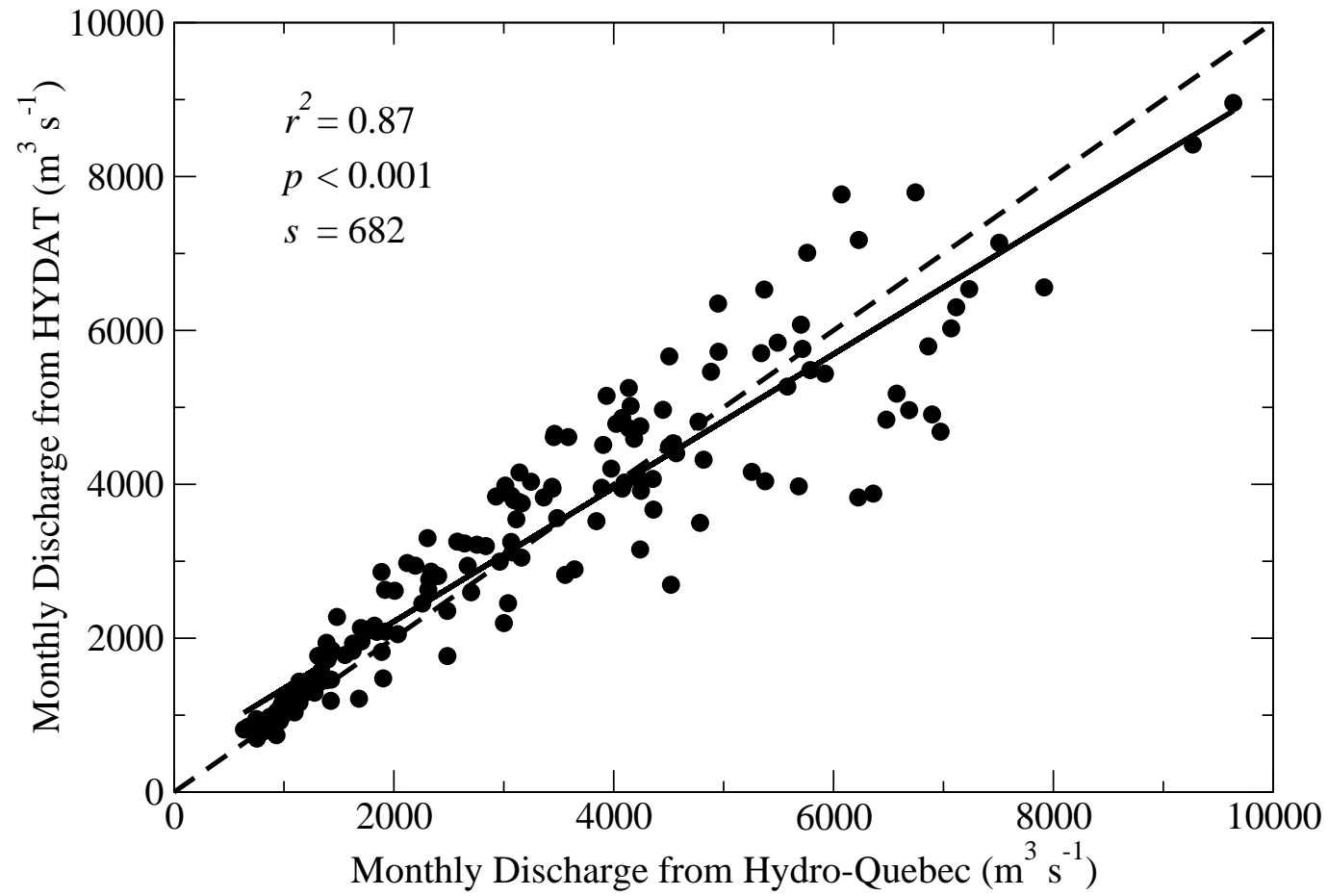


FIGURE 2: Comparison of the monthly discharge rates for La Grande Rivière inferred from Hydro-Québec and from HYDAT, 1981-94. The solid line is the linear regression and the dashed is line the 1:1 line. The coefficient of determination (r^2), probability value (p), and standard error (s) of the linear regression are also given.

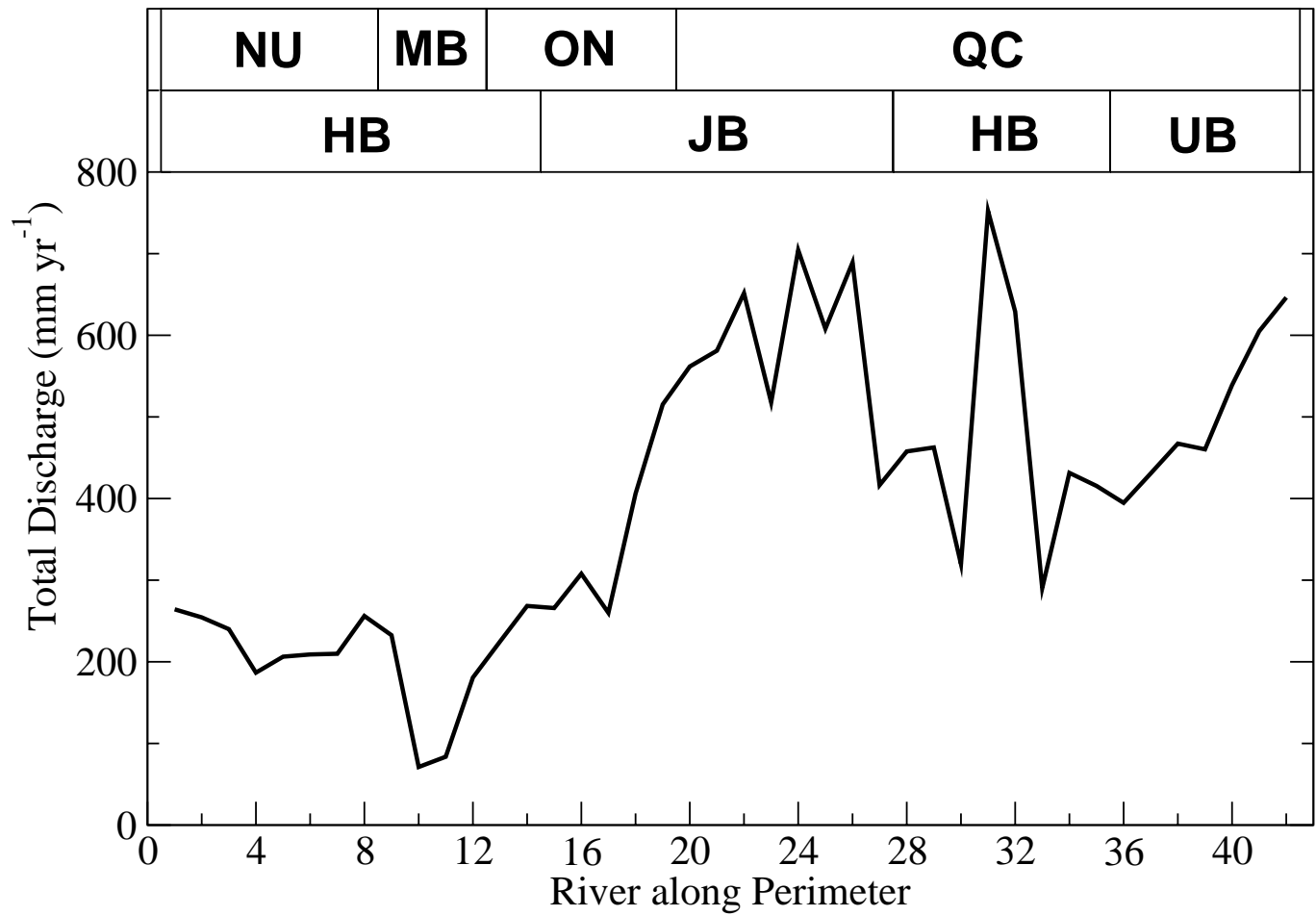


FIGURE 3: The mean annual discharge rates per contributing area for 42 rivers that drain into Hudson Bay (HB), James Bay (HB), and Ungava Bay (UB), 1964-2000. The order of the rivers along the perimeter of the drainage basin is given in Table 7. The province or territory where the mouths of the rivers are located is also provided. The following abbreviations are used: NU, Nunavut; MB, Manitoba; ON, Ontario; QC, Québec.

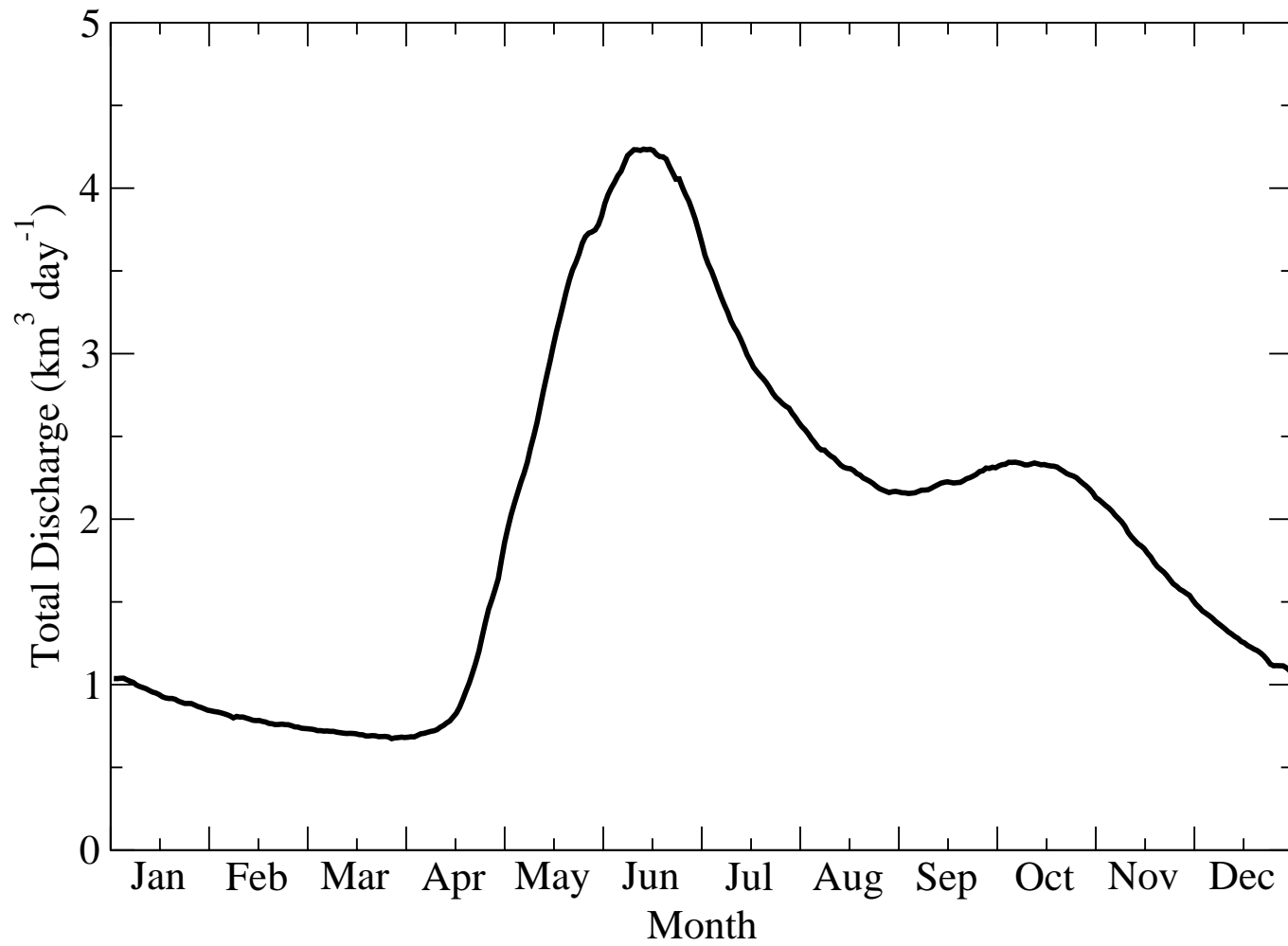


FIGURE 4: The annual cycle of freshwater discharge for 42 rivers that drain into Hudson, James, and Ungava Bays, 1964-2000.

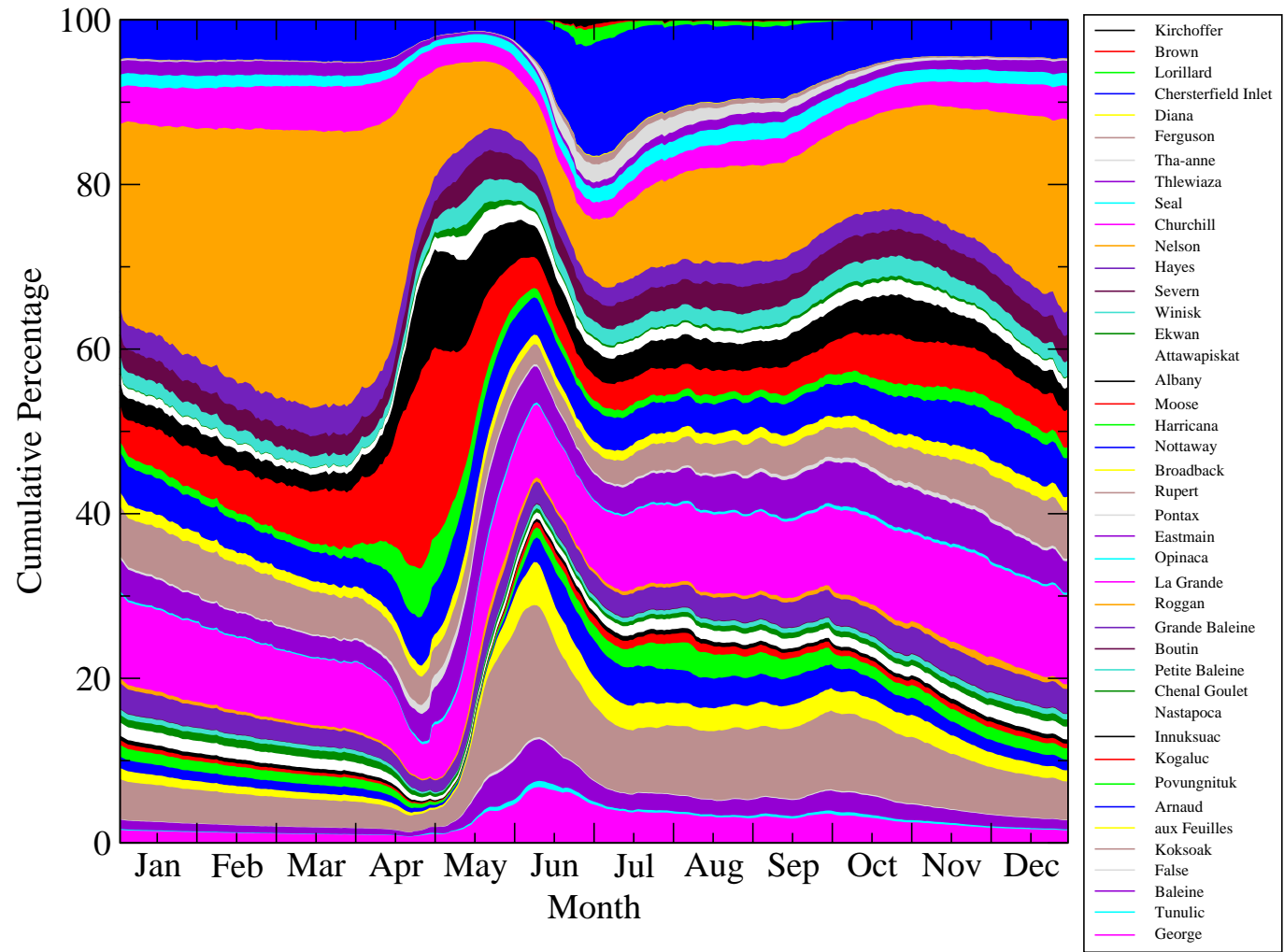


FIGURE 5: The daily contribution (as a cumulative percentage) of 42 rivers to the freshwater discharge into Hudson, James, and Ungava Bays, 1964-2000.

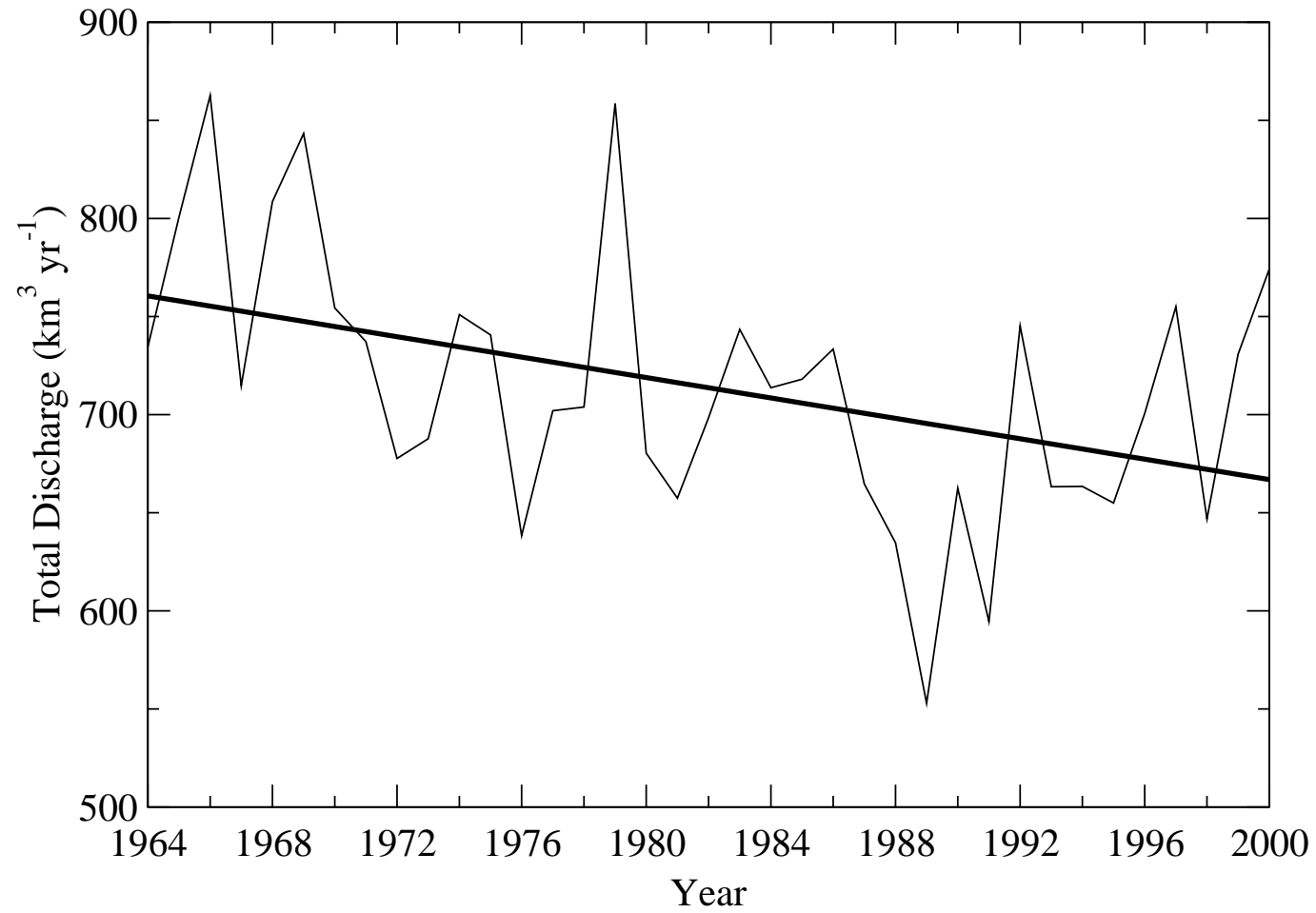


FIGURE 6: The temporal evolution of the total annual freshwater discharge of 42 rivers that drain into Hudson, James, and Ungava Bays, 1964-2000. The thick solid line denotes the Kendall-Theil Robust Line.

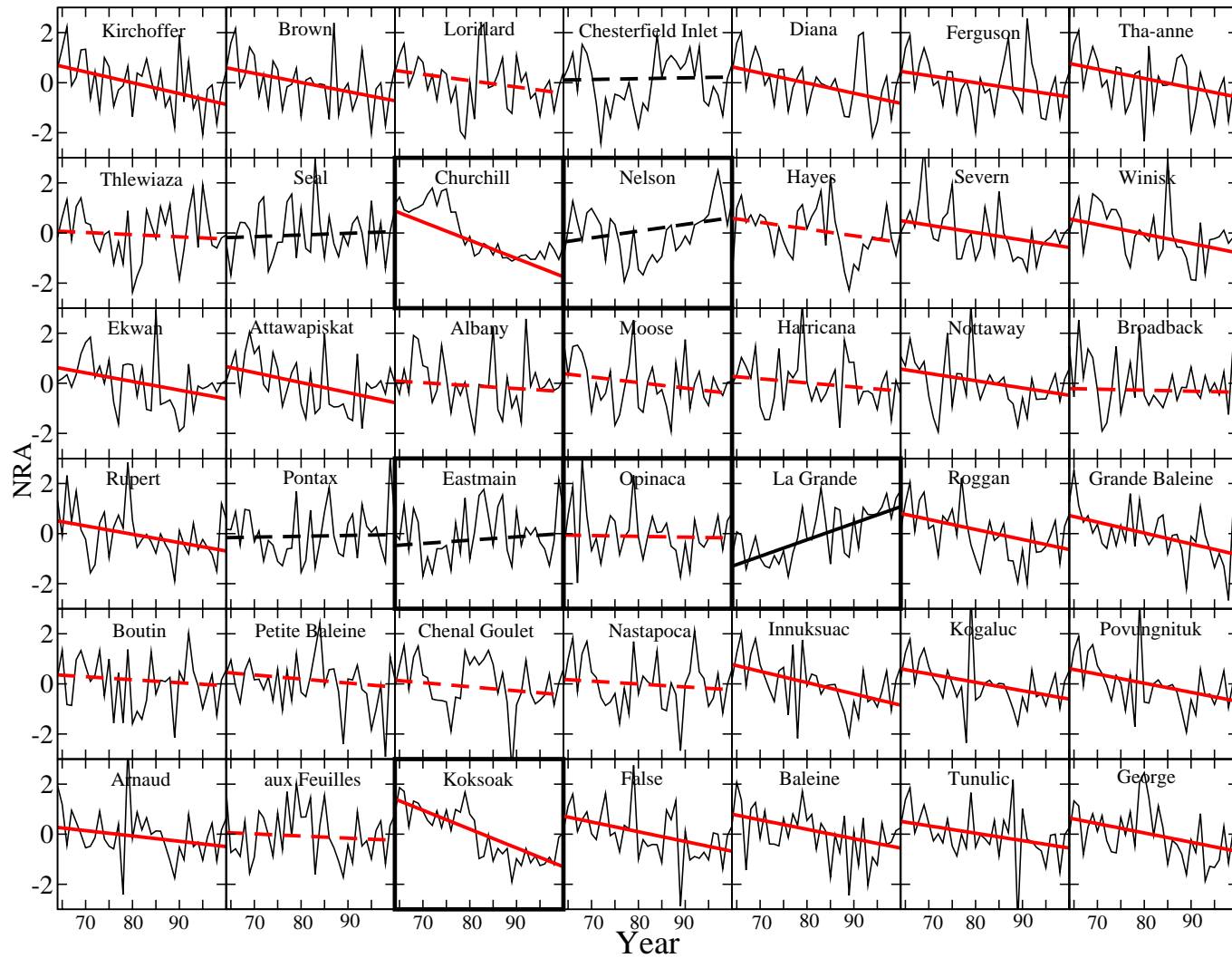


FIGURE 7: The temporal evolution of the annual normalized runoff anomalies (NRA) for 42 rivers that drain into Hudson, James, and Ungava Bays, 1964-2000. The Kendall-Theil Robust lines are included as thick black (red) lines to indicate positive (negative) trends in freshwater discharge. Thick solid (dashed) lines denote rivers with (without) significant trends at the $p < 0.05$ level. Bold frames denote rivers affected by dams, diversions, and/or reservoirs.

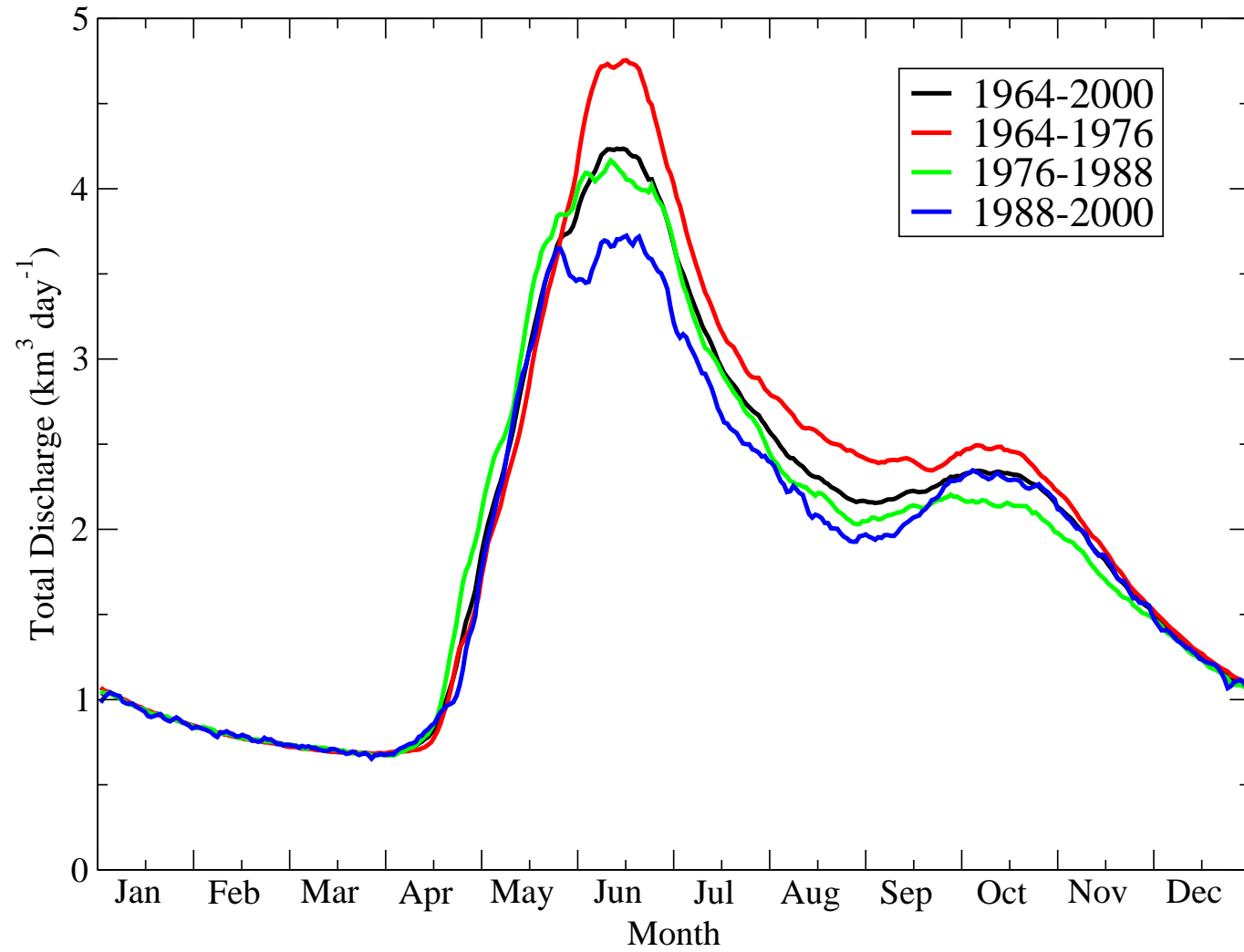


FIGURE 8: The annual cycle of freshwater discharge for 42 rivers that drain into Hudson, James, and Ungava Bays, over four selected time periods.

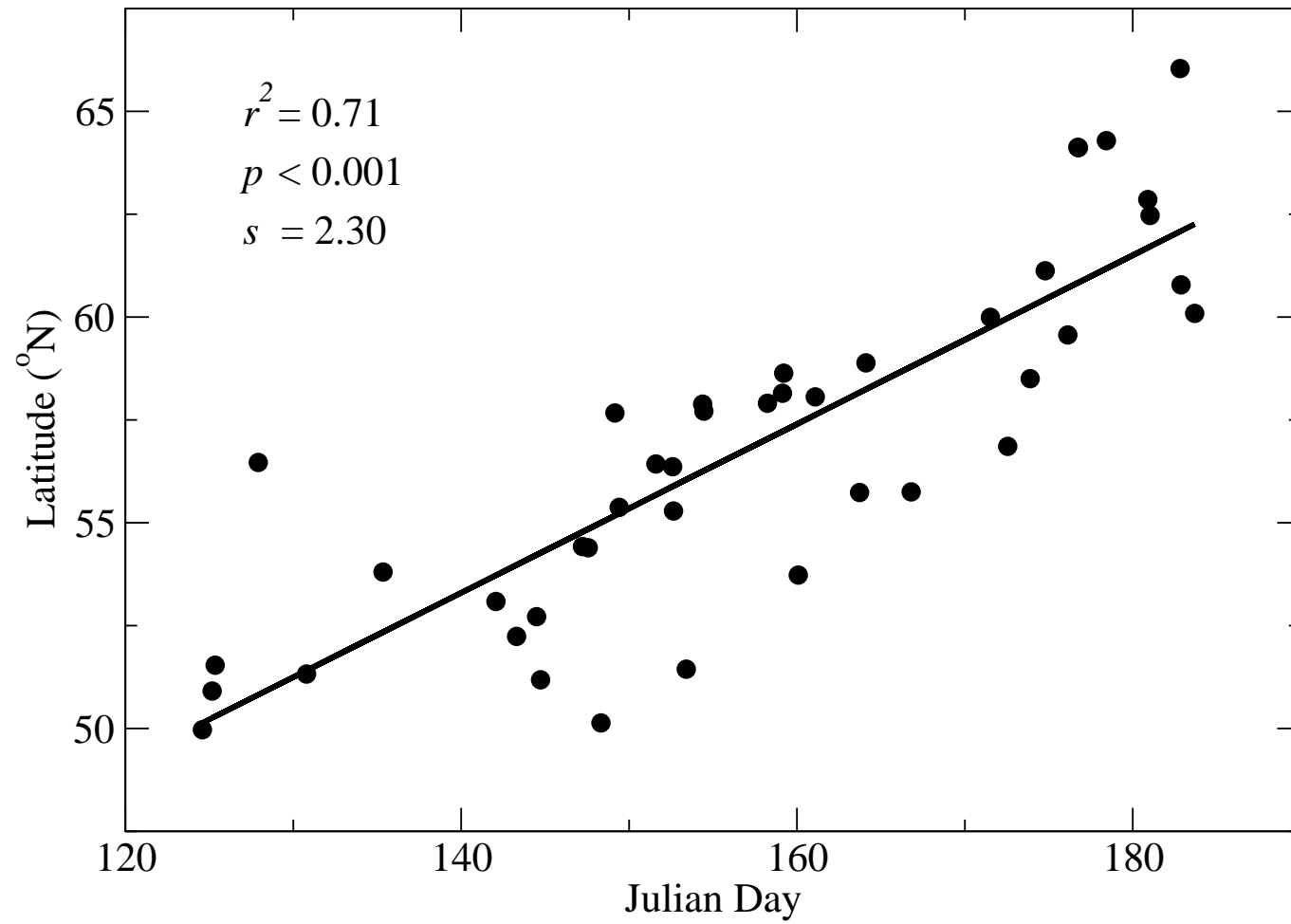


FIGURE 9: The relationship between the date of maximum discharge rate versus the latitude for 42 rivers that drain into Hudson, James, and Ungava Bays, 1964-2000. The coefficient of determination (r^2), probability value (p), and standard error (s) of the linear regression (solid line) are also given.

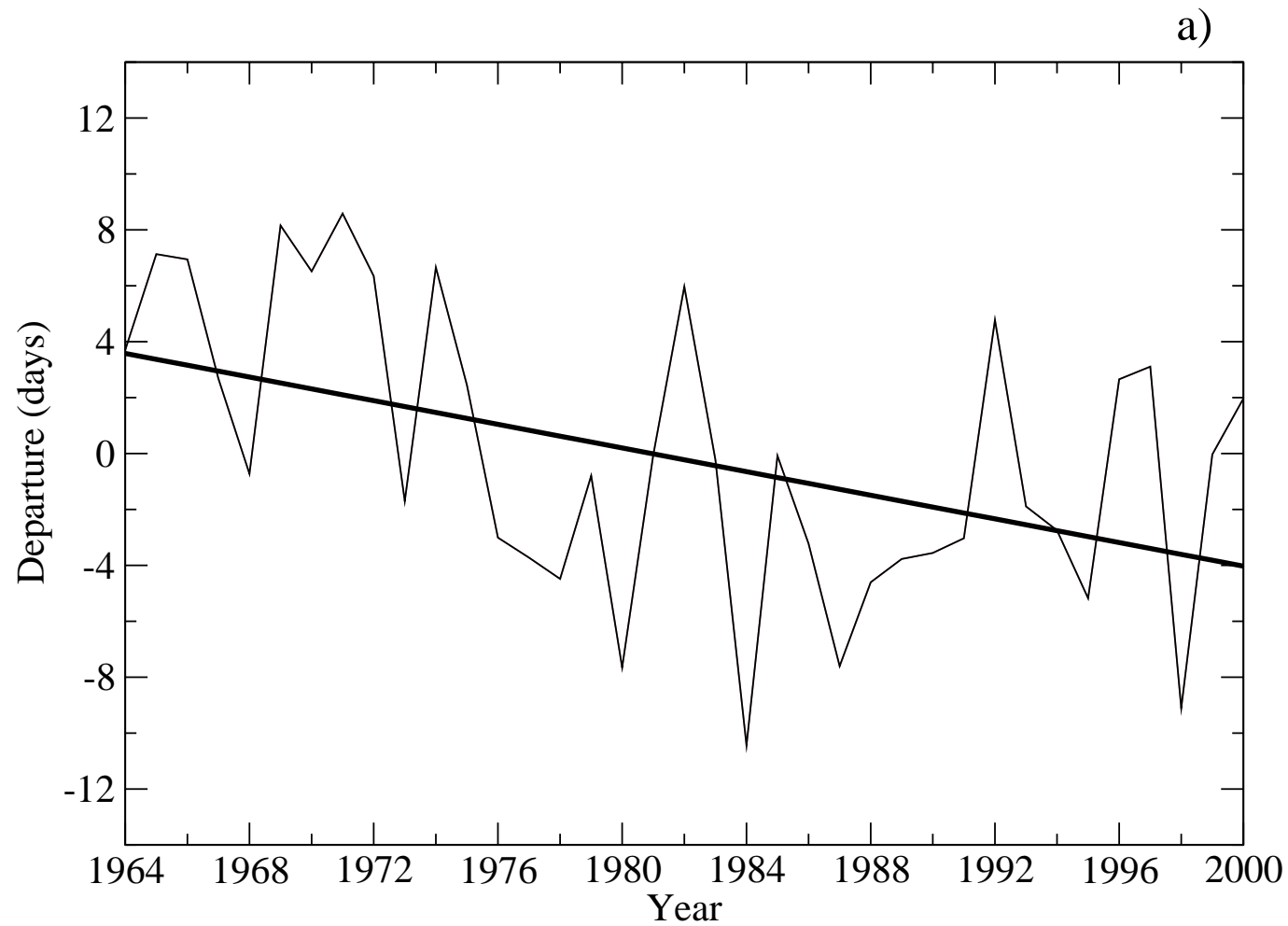
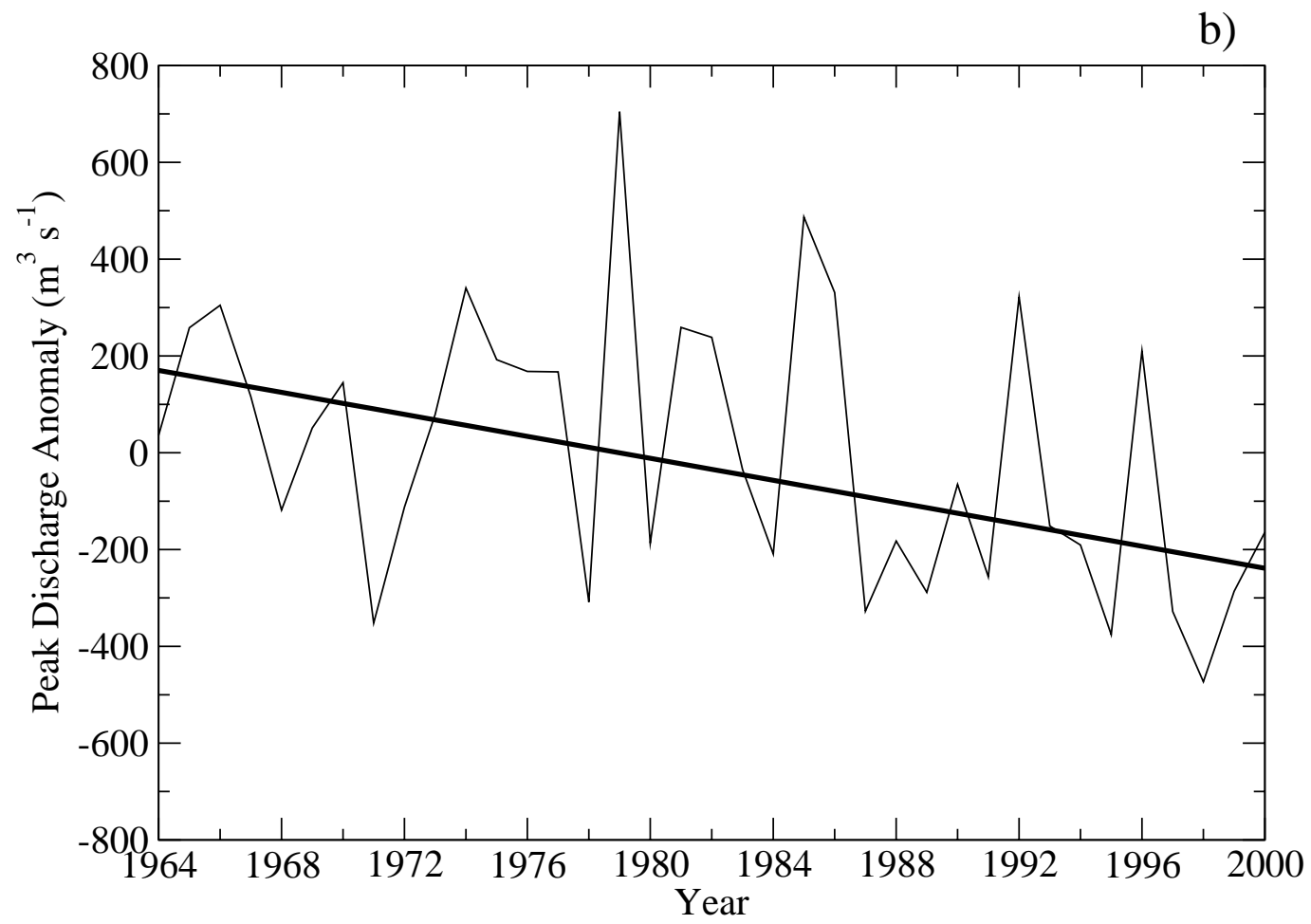


FIGURE 10: The trend in a) the mean departure (in days) from the annual spring maximum discharge rates and in b) the annual spring peak discharge rate anomalies for 42 rivers that drain into Hudson, James, and Ungava Bays, 1964-2000. The thick black lines denote the Kendall-Theil Robust Lines.



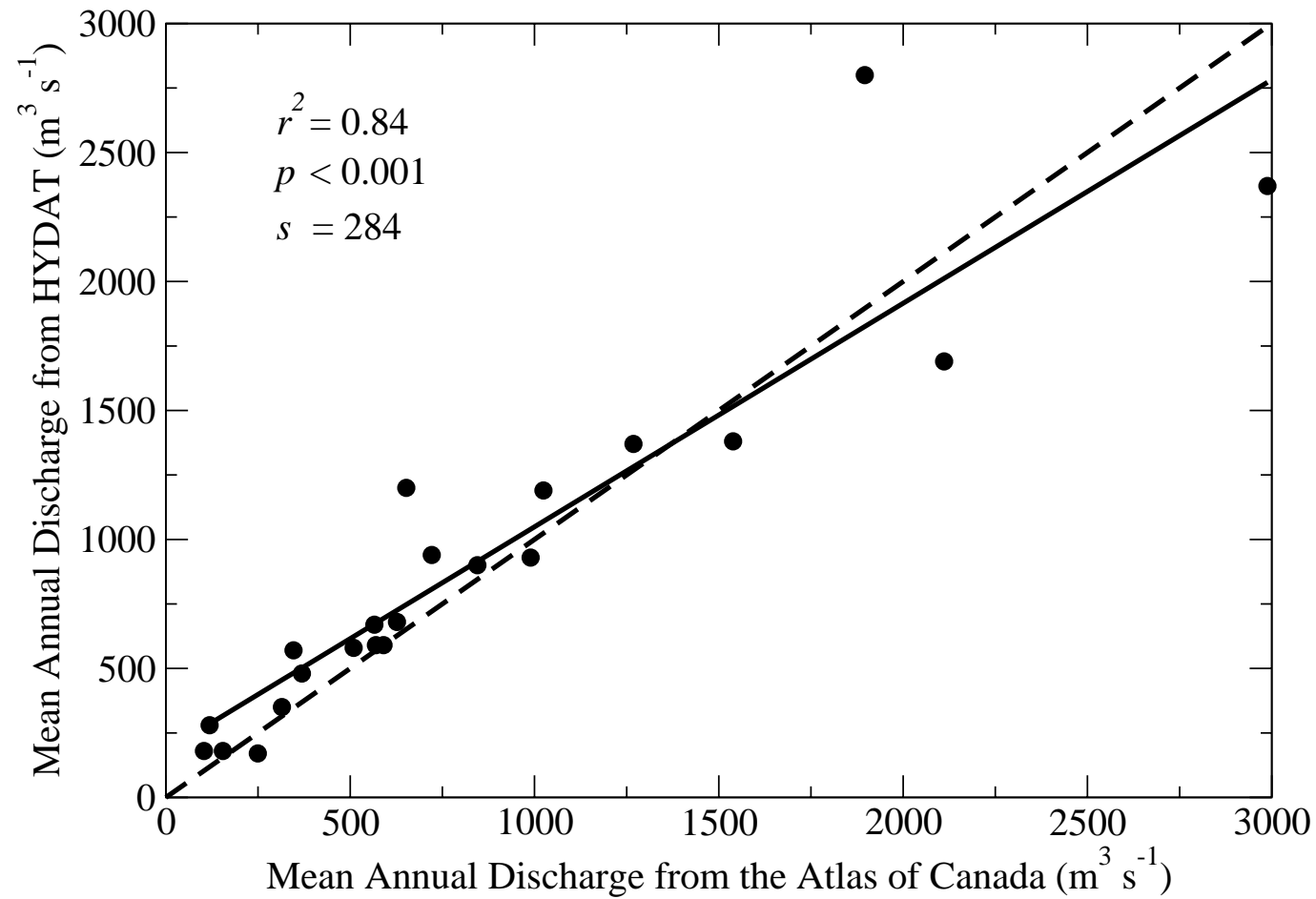


FIGURE 11: Comparison of the annual discharge rates for 22 rivers that drain into Hudson, James, and Ungava Bays from the *Atlas of Canada* versus the results of this study. The solid line is the linear regression and the dashed is line the 1:1 line. The coefficient of determination (r^2), probability value (p), and standard error (s) of the linear regression are also given.

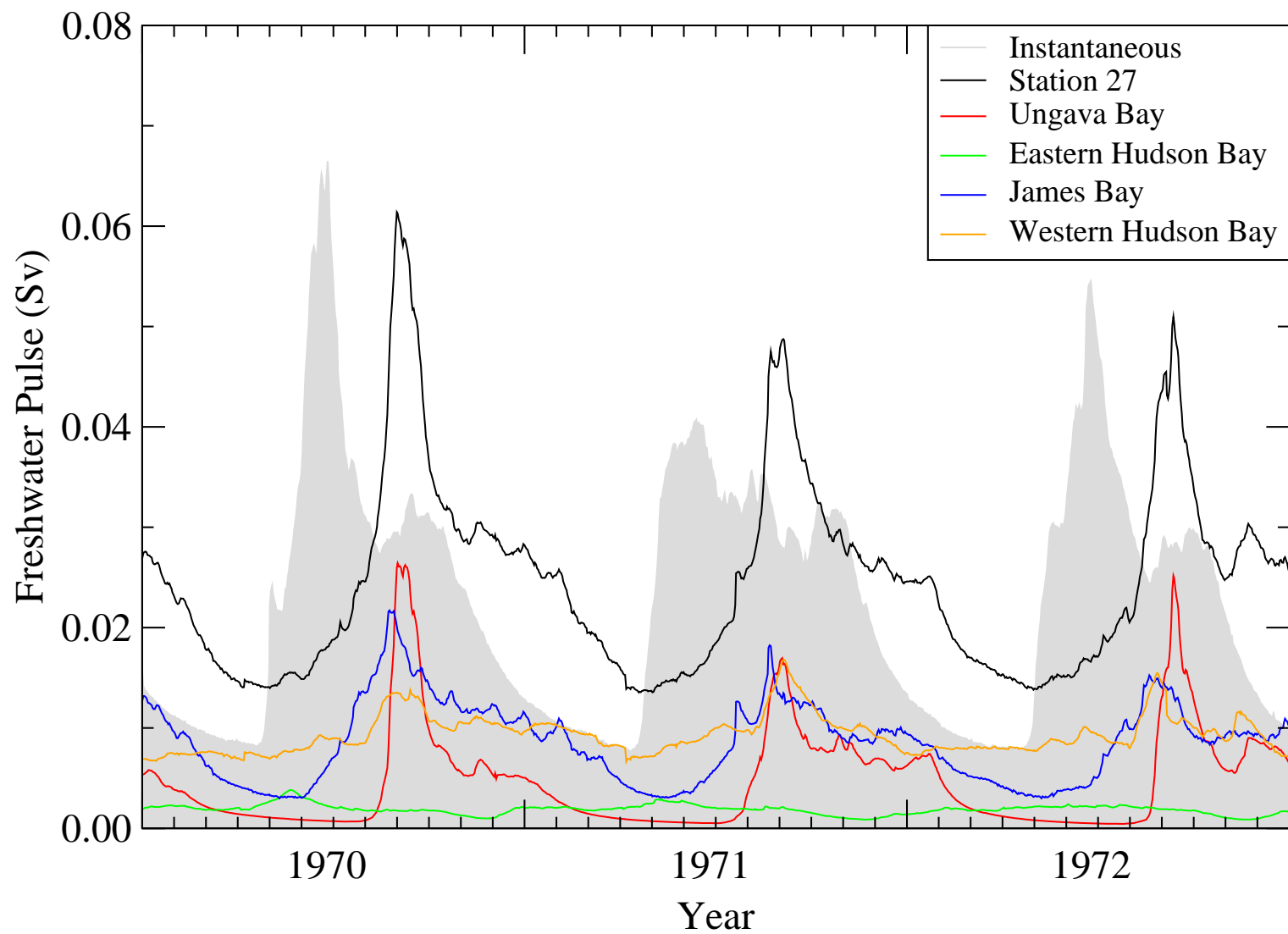


FIGURE 12: The instantaneous daily discharge rates for HJUBs as well as the contribution of four regions along the perimeter of Hudson Bay, James Bay, and Ungava Bay to the total daily freshwater pulse inferred for Station 27 on the inner Newfoundland Shelf, 1970-72.

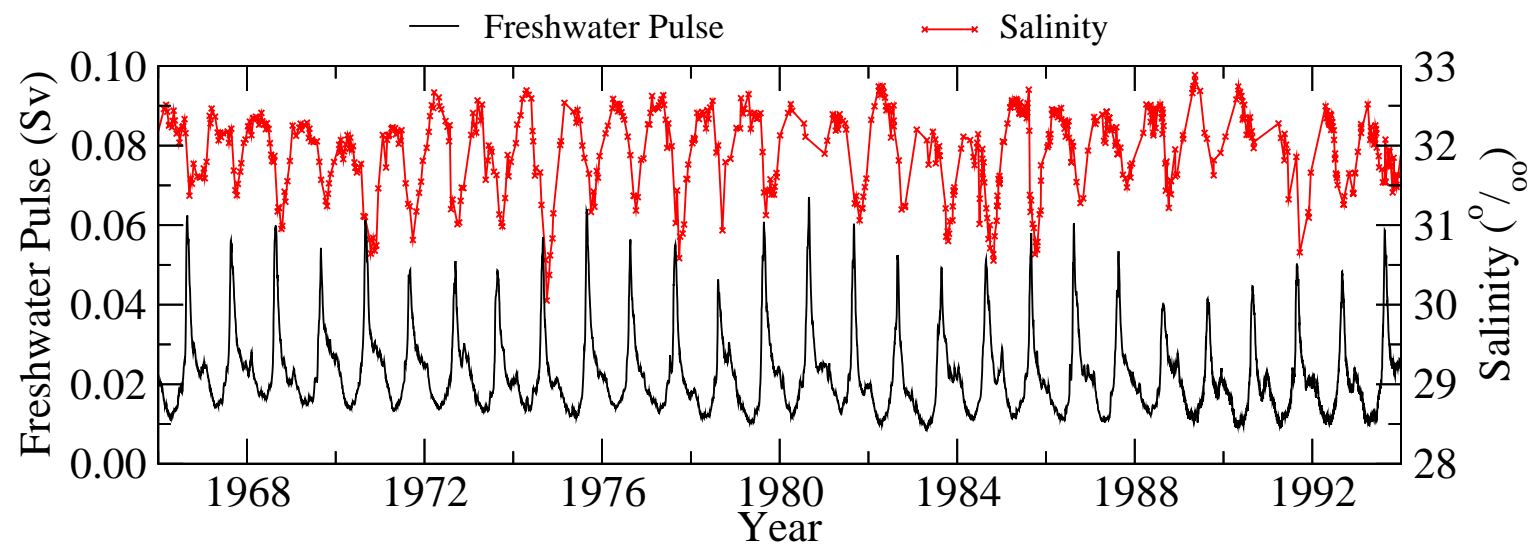


FIGURE 13: The daily freshwater pulse and upper ocean salinity values inferred for Station 27 on the inner Newfoundland Shelf, 1966-94.

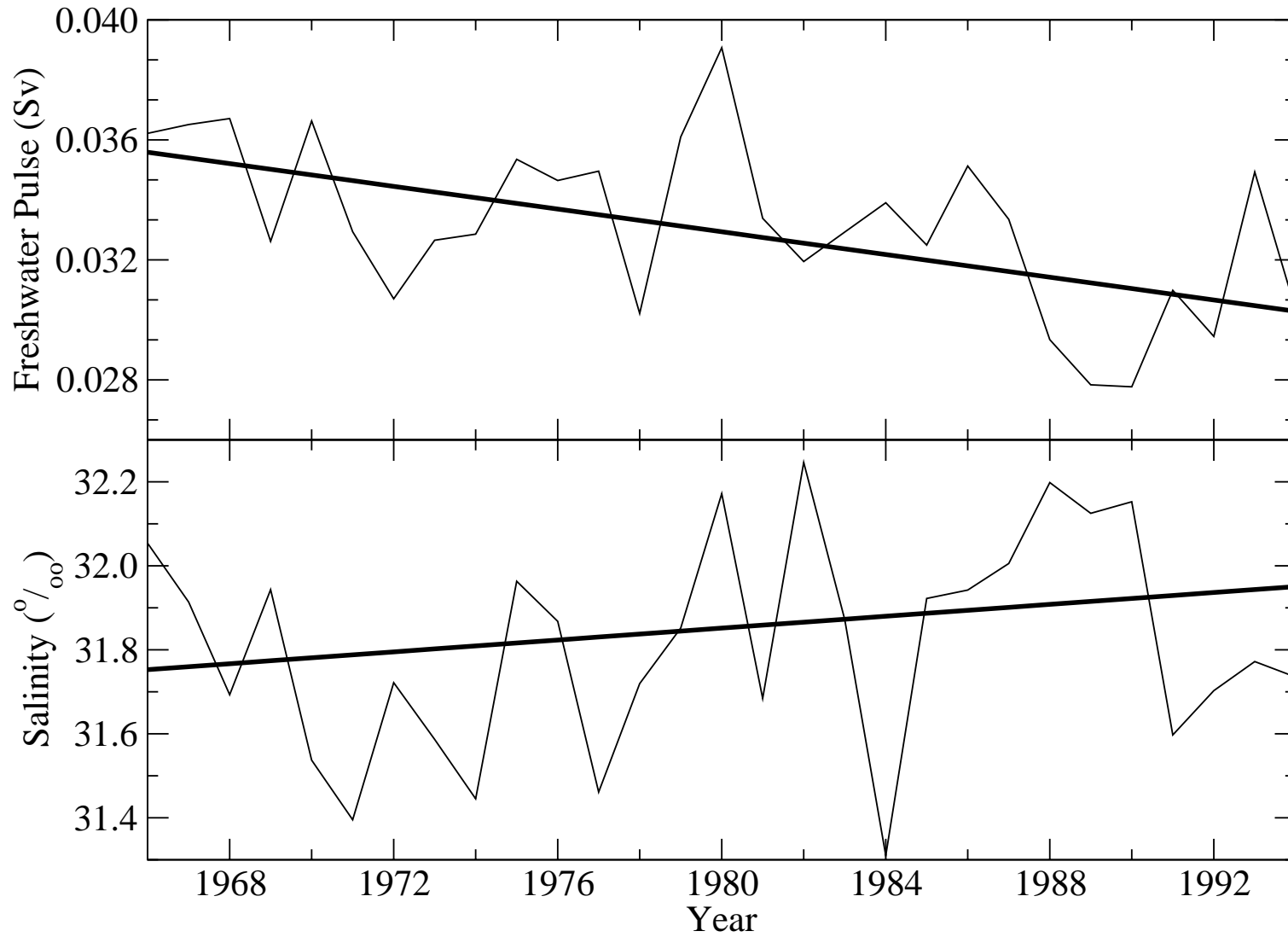


FIGURE 14: The summertime freshwater pulse and upper ocean salinity values inferred for Station 27 on the inner Newfoundland Shelf, 1966-94. The thick black lines denote the Kendall-Theil Robust Lines.

TABLE 1: Alphabetical list of 42 rivers that discharge into Hudson Bay (HB), James Bay (JB), and Ungava Bay (UB), their outlet, province or territory, geographical coordinates of the recording gauge nearest to the mouth, and contributing area that is gauged. The following abbreviations are used: NU, Nunavut Territory; MB, Manitoba; ON, Ontario; QC, Québec.

River	Out- let	Prov./ Terr.	Lat. (°N)	Lon. (°W)	Area (km ²)
Albany	JB	ON	51.33	83.84	118000.
Arnaud	UB	QC	59.98	71.91	45200.
Attawapiskat	JB	ON	53.09	85.01	36000.
à la Baleine	UB	QC	57.88	67.58	29800.
Boutin	HB	QC	55.75	75.83	1390.
Broadback	JB	QC	51.18	77.43	17100.
Brown	HB	NU	66.04	91.83	2040.
Chenal Goulet	HB	QC	56.19	75.54	5970.
Chesterfield Inlet	HB	NU	63.70	90.62	259979.
Churchill	HB	MB	58.12	94.62	288880.
Diana	HB	NU	62.86	92.41	1460.
Eastmain	JB	QC	52.24	78.07	44300.
Ekwan	JB	ON	53.80	84.92	10400.
False	UB	QC	57.67	68.27	2140.
Ferguson	HB	NU	62.47	95.05	12400.
aux Feuilles	UB	QC	58.64	70.42	41700.
George	UB	QC	58.15	65.84	35200.
Grande Rivière de la Baleine	HB	QC	55.29	77.59	43200.
Harricana	JB	QC	49.95	78.72	21200.
Hayes	HB	MB	56.43	92.79	103000.
Innuksuac	HB	QC	58.51	77.96	11200.

River	Out- let	Prov./ Terr.	Lat. (°N)	Lon. (°W)	Area (km ²)
Kirchoffer	HB	NU	64.12	83.44	3160.
Kogaluc	HB	QC	59.57	77.24	11300.
Koksoak	UB	QC	58.02	68.48	110136.
La Grande Rivière	JB	QC	53.72	78.57	96600.
Lorillard	HB	NU	64.29	90.44	11000.
Moose	JB	ON	50.81	81.29	98530.
Nastapoca	HB	QC	56.86	76.21	12500.
Nelson	HB	MB	56.37	94.63	1125520.
Nottaway	JB	QC	50.13	77.42	57500.
Opinaca	JB	QC	52.72	75.99	3700.
Petite Rivière de la Baleine	HB	QC	55.73	74.69	11700.
Pontax	JB	QC	51.53	78.09	6090.
de Povungnituk	HB	QC	60.09	76.94	28000.
Roggan	JB	QC	54.42	79.34	9560.
Rupert	JB	QC	51.44	76.86	40900.
Seal	HB	MB	58.89	96.27	48100.
Severn	HB	ON	55.37	88.32	94300.
Tha-anne	HB	NU	61.00	97.02	29400.
Thlewiaza	HB	NU	60.78	98.77	27000.
Tunulic	UB	QC	57.91	66.37	3680.
Winisk	HB	ON	54.52	87.23	54710.
Total	3013945.

TABLE 2: The mean annual conditions of air temperature (T), precipitation (P), and snowfall (S_f) at selected meteorological stations within the HJUBs drainage system for the period 1971-2000¹.

Station	Prov./ Terr.	Lat. (°N)	Lon. (°W)	Elev. (m)	T (°C)	P (mm)	S_f (mm swe)
Baker Lake	NU	64.30	96.08	18	-11.8	270	114
Big Trout Lake	ON	53.83	89.87	219	-2.7	609	211
Calgary	AB	51.12	114.02	1077	4.1	321	92
Churchill	MB	58.73	94.07	28	-6.9	432	167
Coral Harbour	NU	64.20	83.37	64	-11.6	286	131
Edmonton	AB	54.30	113.58	715	2.4	483	108
Inukjuak	QC	58.45	78.12	3	-7.0	460	195
Kapuskasing	ON	49.42	82.47	226	0.7	832	287
Kuuujuaq	QC	58.45	68.42	34	-5.7	527	250
Moosonee	ON	51.27	80.65	10	-1.1	682	188
Prince Albert	SK	53.22	105.68	428	0.9	424	101
Saskatoon	SK	52.17	106.68	501	2.2	350	85
Schefferville	QC	54.80	66.82	522	-5.3	823	415
The Pas	MB	53.97	101.10	271	0.1	443	119
Winnipeg	MB	50.90	97.23	239	2.6	514	98

¹ Source: Environment Canada (2004a), Canadian Climate and Water Information [http://www.msc-smc.ec.gc.ca/climate/climate_normals_1990/index_e.cfm]

TABLE 3: Error analysis for the reconstructed (REC) river discharge compared to observations (OBS). The analysis is based on the mean daily values of river runoff between 18 June 1974 and 5 July 1988 for the Petite Rivière de la Baleine. Two reconstructions are presented: one based on upstream measurements (REC1) and the other based on the remaining available discharge data (REC2). The following abbreviations are used: r^2 , coefficient of determination; MAE, mean absolute error; RMSE, root mean square error.

Dataset	Mean ($\text{m}^3 \text{ s}^{-1}$)	r^2	MAE ($\text{m}^3 \text{ s}^{-1}$)	RMSE ($\text{m}^3 \text{ s}^{-1}$)
OBS	123.1
REC1	115.4	0.97	10.6	0.20
REC2	117.2	0.82	20.9	0.43

TABLE 4: List of HJUBs rivers that are affected by major dams, diversions (div), and/or reservoirs (res) as well as the approximate year when major human impacts began.

River	Human Impact	Year
Churchill	div	1976/77
Eastmain	div	1980
Koksoak	div	1982
La Grande Rivière	dam, res	1980
Moose	dam	<1964
Nelson	dam	<1964
Opinaca	div	1980

TABLE 5: Annual discharge rates for 42 rivers that drain into Hudson, James, and Ungava Bays. The mean peak flow induced by meltwater and the julian day at which it occurs are also listed.

Rank	River	Discharge				Peak	Day of
		(km ³ yr ⁻¹)	($\times 10^{-3}$ Sv)	(%)	(mm yr ⁻¹)	Flow (m ³ s ⁻¹)	Peak Flow
1	Nelson	94.24	2.986	13.21	83.7	4110.3	128
2	La Grande ¹	66.57	2.110	9.33	689.2	4961.7	160
3	Koksoak	59.79	1.895	8.38	467.4	10275.5	154
4	Chesterfield Inlet	48.52	1.538	6.80	186.7	6616.9	177
5	Moose	40.00	1.268	5.61	406.0	7459.5	125
6	Nottaway	32.30	1.024	4.53	561.7	2784.4	148
7	Eastmain	31.20	0.989	4.37	704.3	3266.7	143
8	Albany	30.69	0.972	4.30	260.1	4368.7	131
9	Rupert	26.65	0.845	3.73	651.6	1328.5	153
10	George	22.75	0.721	3.19	646.3	4437.6	159
11	Severn	21.20	0.672	2.97	224.8	1983.0	149
12	Churchill	20.57	0.652	2.88	71.2	1320.1	161
13	Grande Rivière						
	de la Baleine	19.77	0.627	2.77	457.6	1735.7	153
14	Hayes	18.62	0.590	2.61	180.7	1944.1	152
15	aux Feuilles	17.96	0.569	2.52	430.8	3420.2	159
16	Arnaud	17.84	0.565	2.50	394.7	2655.3	172
17	à la Baleine	16.06	0.509	2.25	539.0	3470.3	154
18	Winisk	14.69	0.466	2.06	268.5	1561.6	148
19	de Povungnituk	11.63	0.369	1.63	415.4	869.8	184
20	Seal	11.19	0.355	1.57	232.6	936.8	164
21	Attawapiskat	11.08	0.351	1.55	307.9	1315.7	142
22	Harricana	10.92	0.346	1.53	515.3	1727.1	125

Rank	River	Discharge				Peak	Day of
		(km ³ yr ⁻¹)	(×10 ⁻³ Sv)	(%)	(mm yr ⁻¹)	Flow (m ³ s ⁻¹)	Peak Flow
23	Broadback	9.94	0.315	1.39	581.1	768.1	145
24	Nastapoca	7.86	0.249	1.10	629.0	483.3	173
25	Thlewiaza	6.92	0.219	0.97	256.2	334.5	183
26	Tha-anne	6.17	0.196	0.86	209.9	1049.9	175
27	Kogaluc	4.88	0.155	0.68	431.4	485.1	176
28	Chenal Goulet	4.49	0.142	0.63	752.3	289.6	153
29	Roggan	3.98	0.126	0.56	416.4	551.8	147
30	Petite Rivière						
	de la Baleine	3.74	0.119	0.52	319.8	288.9	164
31	Innuksuac	3.25	0.103	0.46	290.2	295.2	174
32	Pontax	3.15	0.100	0.44	517.9	500.1	125
33	Ekwan	2.76	0.088	0.39	265.8	611.0	135
34	Lorillard	2.64	0.084	0.37	239.9	1131.5	178
35	Ferguson	2.59	0.082	0.36	209.0	413.8	181
36	Opinaca	2.25	0.071	0.32	607.9	263.2	144
37	Tunulic	2.23	0.071	0.31	605.0	490.7	158
38	False	0.99	0.031	0.14	460.3	204.2	149
39	Kirchoffer	0.84	0.027	0.12	264.2	491.7	177
40	Boutin	0.64	0.020	0.09	462.5	74.2	167
41	Brown	0.52	0.016	0.07	254.4	240.6	183
42	Diana	0.30	0.010	0.04	206.3	56.6	181
	Total	713.6	22.614	100.00%	235.4

¹ The combined freshwater discharge of the La Grande, Opinaca, and Eastmain Rivers totals 100.02 km³ yr⁻¹. As a result of river diversions, the discharge of La Grande Rivière surpasses that of the Nelson River after 1980.

TABLE 6: Contribution of each bay and of each province or territory to the total freshwater discharge in Hudson, James and Ungava Bays over the period 1964-2000.

Bay	Area (%)	Discharge (%)	Province/ Territory	Area (%)	Discharge (%)
Hudson	72.1	42.7	Manitoba	51.6	20.2
James	18.5	38.0	Nunavut	11.4	9.6
Ungava	9.4	19.3	Ontario	13.9	17.6
			Québec	23.0	52.6
Total	100.0	100.0	Total	100.0	100.0

TABLE 7: The delay (in days) it takes for freshwater discharge from 42 rivers along the perimeter of Hudson Bay, James Bay, and Ungava Bay, to reach Station 27 (47.5°N, 52.6°W) on the inner Newfoundland Shelf. The approximate distance between the mouth of the rivers to Station 27 and the julian day at which peak discharge rates associated with meltwater reaches this destination are also indicated. Bold values indicate peak freshwater pulses arriving at Station 27 on average between 1 July and 31 September of each year.

Order along perimeter	River	Delay to Station 27 (days)	Distance to Station 27 (km)	Day of peak flow at Station 27
1	Kirchoffer	874	2950	320
2	Brown	889	2987	341
3	Lorillard	817	2802	265
4	Chesterfield Inlet	792	2736	238
5	Diana	752	2632	202
6	Ferguson	747	2619	198
7	Tha-anne	697	2489	141
8	Thlewiaza	691	2475	143
9	Seal	676	2437	110
10	Churchill	635	2328	66
11	Nelson	627	2309	7
12	Hayes	584	2197	5
13	Severn	461	1877	245
14	Winisk	399	1717	181
15	Ekwan	413	1810	183
16	Attawapiskat	423	1843	200
17	Albany	445	1919	210
18	Moose	476	2027	236
19	Harricana	472	2013	231

Order along perimeter	River	Delay to Station 27 (days)	Distance to Station 27 (km)	Day of peak flow at Station 27
20	Nottaway	471	2008	254
21	Broadback	471	2008	250
22	Rupert	464	1986	252
23	Pontax	459	1970	219
24	Eastmain	437	1891	215
25	Opinaca	438	1895	217
26	La Grande	389	1726	184
27	Roggan	368	1652	150
28	Grande Rivière de la Baleine	339	1552	126
29	Boutin	317	1476	118
30	Petite Rivière de la Baleine	317	1476	115
31	Chenal Goulet	301	1421	88
32	Nastapoca	290	1386	97
33	Innuksuac	235	1194	43
34	Kogaluc	201	1078	12
35	de Povungnituk	185	1023	3
36	Arnaud	72	299	243
37	aux Feuilles	84	409	243
38	Koksoak	82	389	236
39	False	85	418	234
40	à la Baleine	81	379	235
41	Tunulic	78	353	236
42	George	74	320	233